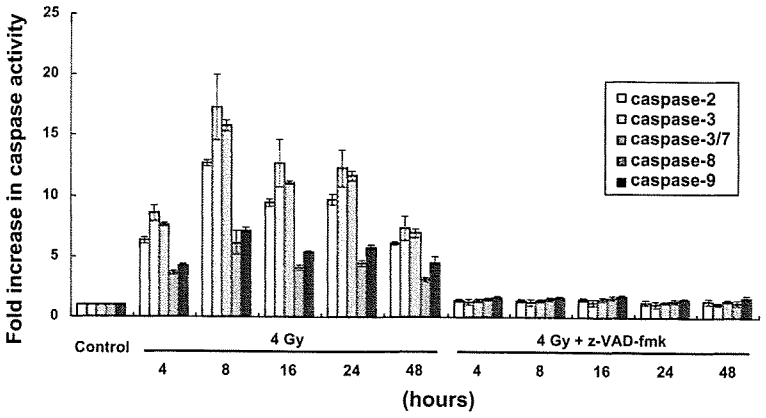

Fig. 5. Caspase activity of irradiated MOLT-4 cells in the absence or presence of a caspase inhibitor. Activities of caspases 2, 3, 3/7, 8, and 9 were examined by colorimetric assay with or without a pretreatment with 100 μM z-VAD-fmk, using fluorogenic substrates for these caspases. Fold increases in caspase activities are shown, compared with unirradiated control cells. An average of two measurements is used.

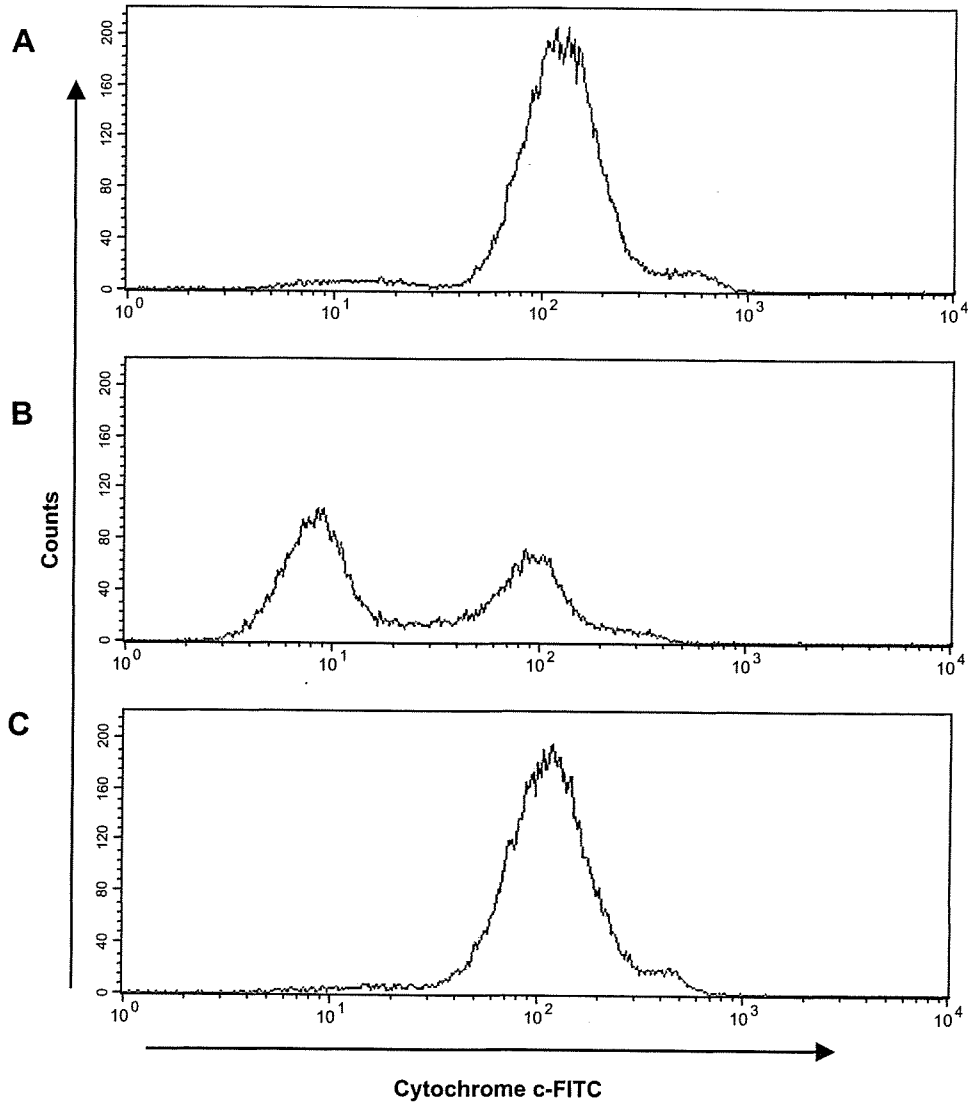

Fig. 6. Release of cytochrome *c* from mitochondria in irradiated MOLT-4 cells. Mitochondrial cytochrome *c* was detected by using anti-cytochrome *c* antibody (clone 7H8.2C12) in fixed and permeabilized MOLT-4 cells. This antibody binds only to mitochondrial cytochrome *c*, not to cytosolic one. Cells were gated according to forward/side scatter properties into viable or early phase of cell death, and then analyzed by flow-cytometry. (A) Unirradiated MOLT-4 cells. (B) MOLT-4 cells at 16 h after a 4 Gy irradiation. (C) MOLT-4 cells at 16 h after a 4 Gy irradiation in the presence of 100 μM z-VAD-fmk.

the cells were pretreated with z-VAD-fmk (Fig. 6C). These results suggest that the release of cytochrome c might not invariably precede necrotic cell death in irradiated MOLT-4.

4. Discussion

In the present study, apoptotic cell death was induced by a 4 Gy irradiation in MOLT-4, a thymus-derived T cell line, and the apoptosis was characterized by a decrease in mitochondrial membrane potential and an increase in intracellular ROS. On the one hand, when caspase activities were suppressed by the z-VAD-fmk pretreatment, irradiated MOLT-4 avoided apoptosis, and died exhibiting necrotic features. We demonstrated for the first time that there was no increase in intracellular ROS in the process of this necrotic cell death of MOLT-4. These results indicate that apoptosis, as the main pathway of radiation-induced cell death in MOLT-4, requires both elevation of intracellular ROS and activation of a series of caspases, while the cryptic necrosis program—independent of ROS generation and caspase activation—becomes active when the apoptosis pathway is blocked.

In agreement with our observations, this shift from apoptosis to necrosis has been reported in several cell types when the apoptosis pathways were blocked by z-VAD-fmk (U-937 cell death induced by camptothecin [24], mouse thymocyte death induced by dexamethasone and etoposide [7], and irradiated MOLT-4 cell death [8]). Enhanced expression of Bcl-2 also generated a similar shift from apoptosis to necrosis in HL-60 cells treated with oxidized low density lipoproteins [25]. In addition, interdigital cells from mice genetically lacking the caspase activator Apaf-1 underwent necrosis, not apoptosis, during embryonic development [26]. Therefore, it is plausible to imagine that cell death, including radiation-induced death, can be achieved through multiple molecular pathways—typically apoptotic or necrotic—depending on cellular physiological status and available effecter molecules.

Previous studies on radiation-induced apoptosis in MOLT-4 have suggested involvement of individual intracellular events (mediation by p53, activation of SAPK/JNK pathway, critical roles for caspase-3, modulation by Bcl-2, and occurrence of ceramide formation and PARP cleavage [8,21,23,27–29]). Even so, the sequential process of apoptosis still remains to be clarified. That is why we analyzed the temporal process of cell death in terms of mitochondrial membrane potential and intracellular ROS in this study. Our time-course analyses indicate that excess generation of ROS precedes the reduction of the membrane potential during radiation-induced apoptosis in MOLT-4 cells, whereas ROS generation is bypassed during radiation-induced necrosis. Given the potential implications of our findings, the use of antioxidants is indeed a promising strategy for prevention of radiation-induced, and ROS-dependent, cell death upon the development of radioprotective agents for cancer radiotherapy [30]. However, our findings also imply that antioxidants as radioprotective agents may be less effective for ROS-independent necrosis. Thus, development of radioprotective strategies that take into account the molecular mechanisms of ROS-independent necrosis is also warranted.

The precise mechanisms of necrosis in MOLT-4 cells remain unclear. Some previous studies have suggested the involvement of intracellular ROS generation during caspase-independent necrotic cell death, e.g., in neutrophil cells [22,31], while our and other studies have observed unaltered levels of ROS [32,33]. This discrepancy regarding ROS generation in necrotic cell death could be due to different types of cells or different experimental procedures used to induce cell death. This would imply that there are multiple pathways even in caspase-independent necrosis, both ROS-dependent and -independent. In fact, a necrotic-signaling pathway involving ROS was thought to be death receptor-mediated [22,34]. That pathway is probably distinct from the necrosis pathway of irradiated MOLT-4 found in this study, because necrosis in MOLT-4 was observed with total suppression of caspase-8, an initiation molecule for the death receptor-mediated pathway.

In addition, several non-caspase proteases, including calpain, cathepsin, and serine protease Omi/HtrA2, have been reported to be major factors in the propagation and execution phases of necrotic cell death, with or without ROS-generation [32,35–37]. Therefore, it seems certain that further studies will be needed to investigate the involvement of these non-caspase proteases in ROS-independent necrotic cell death.

Acknowledgments

The Radiation Effects Research Foundation (RERF), Hiroshima and Nagasaki, Japan is a private, non-profit foundation funded by the Japanese Ministry of Health, Labour and Welfare (MHLW) and the US Department of Energy (DOE), the latter in part through the National Academy of Sciences. This publication was supported by RERF Research Protocol 1-93 and in part by Grant-in-Aid for Scientific Research from the Ministry of Education, Culture, Sports, Science and Technology of Japan, and Grant-in-Aid for Cancer Research from the Ministry of Health, Labour and Welfare of Japan.

References

[1] S.L. Fink, B.T. Cookson, Apoptosis, pyroptosis, and necrosis: mechanistic description of dead and dying eukaryotic cells, Infect. Immun. 73 (2005) 1907–1916.
[2] G. Rainaldi, R. Romano, P. Indovina, A. Ferrante, A. Motta, P.L. Indovina, M.T. Santini, Metabolomics using 1H-NMR of apoptosis and Necrosis in HL60 leukemia cells: differences between the two types of cell death and independence from the stimulus of apoptosis used, Radiat. Res. 169 (2008) 170–180.
[3] G.M. Cohen, Caspases: the executioners of apoptosis, Biochem. J. 326 (Pt 1) (1997) 1–16.
[4] M. Enari, H. Sakahira, H. Yokoyama, K. Okawa, A. Iwamatsu, S. Nagata, A caspase-activated DNase that degrades DNA during apoptosis, and its inhibitor ICAD, Nature 391 (1998) 43–50.
[5] T. Lindsten, A.J. Ross, A. King, W.X. Zong, J.C. Rathmell, H.A. Shiels, E. Ulrich, K.G. Waymire, P. Mahar, K. Frauwirth, Y. Chen, M. Wei, V.M. Eng, D.M. Adelman, M.C. Simon, A. Ma, J.A. Golden, G. Evan, S.J. Korsmeyer, G.R. MacGregor, C.B. Thompson, The combined functions of proapoptotic Bcl-2 family members bak and bax are essential for normal development of multiple tissues, Mol. Cell 6 (2000) 1389–1399.
[6] A. Konishi, S. Shimizu, J. Hirota, T. Takao, Y. Fan, Y. Matsuoka, L. Zhang, Y. Yoneda, Y. Fujii, A.I. Skoultchi, Y. Tsujimoto, Involvement of histone H1.2 in apoptosis induced by DNA double-strand breaks, Cell 114 (2003) 673–688.
[7] T. Hirsch, P. Marchetti, S.A. Susin, B. Dallaporta, N. Zamzami, I. Marzo, M. Geuskens, G. Kroemer, The apoptosis-necrosis paradox. Apoptogenic proteases activated after mitochondrial permeability transition determine the mode of cell death, Oncogene 15 (1997) 1573–1581.
[8] D. Coelho, V. Holl, D. Weltin, T. Lacornerie, P. Magnenet, P. Dufour, P. Bischoff, Caspase-3-like activity determines the type of cell death following ionizing radiation in MOLT-4 human leukaemia cells, Br. J. Cancer 83 (2000) 642–649.
[9] P. Golstein, G. Kroemer, Cell death by necrosis: towards a molecular definition, Trends Biochem. Sci. 32 (2007) 37–43.
[10] J. Minowada, T. Onuma, G.E. Moore, Rosette-forming human lymphoid cell lines. I. Establishment and evidence for origin of thymus-derived lymphocytes, J. Natl. Cancer Inst. 49 (1972) 891–895.
[11] L.B. Chen, Mitochondrial membrane potential in living cells, Annu. Rev. Cell Biol. 4 (1988) 155–181.
[12] J.J. Ubl, J.Y. Chatton, S. Chen, J.W. Stucki, A critical evaluation of in situ measurement of mitochondrial electrical potentials in single hepatocytes, Biochim. Biophys. Acta 1276 (1996) 124–132.
[13] C. Ferlini, G. Scambia, Assay for apoptosis using the mitochondrial probes, Rhodamine123 and 10-N-nonyl acridine orange, Nat. Protoc. 2 (2007) 3111–3114.
[14] G. Rothe, G. Valet, Flow cytometric analysis of respiratory burst activity in phagocytes with hydroethidine and 2′,7′-dichlorofluorescin, J. Leukoc. Biol. 47 (1990) 440–448.
[15] S. Walrand, S. Valeix, C. Rodriguez, P. Ligot, J. Chassagne, M.P. Vasson, Flow cytometry study of polymorphonuclear neutrophil oxidative burst: a comparison of three fluorescent probes, Clin. Chim. Acta 331 (2003) 103–110.
[16] K. Stahnke, A. Mohr, J. Liu, L.H. Meyer, L. Karawajew, K.M. Debatin, Identification of deficient mitochondrial signaling in apoptosis resistant leukemia cells by flow cytometric analysis of intracellular cytochrome c, caspase-3 and apoptosis, Apoptosis 9 (2004) 457–465.

[17] X. Wang, The expanding role of mitochondria in apoptosis, Genes Dev. 15 (2001) 2922–2933.
[18] J.F. Curtin, M. Donovan, T.G. Cotter, Regulation and measurement of oxidative stress in apoptosis, J. Immunol. Methods 265 (2002) 49–72.
[19] P. Tripathi, D. Hildeman, Sensitization of T cells to apoptosis—a role for ROS?, Apoptosis 9 (2004) 515–523
[20] H. Nakano, K. Shinohara, Time sequence analysis of caspase-3-independent programmed cell death and apoptosis in X-irradiated human leukemic MOLT-4 cells, Cell Tissue Res. 310 (2002) 305–311.
[21] O. Inanami, K. Takahashi, M. Kuwabara, Attenuation of caspase-3-dependent apoptosis by Trolox post-treatment of X-irradiated MOLT-4 cells, Int. J. Radiat. Biol. 75 (1999) 155–163.
[22] W.X. Zong, C.B. Thompson, Necrotic death as a cell fate, Genes Dev. 20 (2006) 1–15.
[23] K. Takahashi, O. Inanami, M. Hayashi, M. Kuwabara, Protein synthesis-dependent apoptotic signalling pathway in X-irradiated MOLT-4 human leukaemia cell line, Int. J. Radiat. Biol. 78 (2002) 115–124.
[24] A.T. Sane, R. Bertrand, Caspase inhibition in camptothecin-treated U-937 cells is coupled with a shift from apoptosis to transient G1 arrest followed by necrotic cell death, Cancer Res. 59 (1999) 3565–3569.
[25] O. Meilhac, I. Escargueil-Blanc, J.C. Thiers, R. Salvayre, A. Negre-Salvayre, Bcl-2 alters the balance between apoptosis and necrosis, but does not prevent cell death induced by oxidized low density lipoproteins, Faseb J. 13 (1999) 485–494.
[26] M. Chautan, G. Chazal, F. Cecconi, P. Gruss, P. Golstein, Interdigital cell death can occur through a necrotic and caspase-independent pathway, Curr. Biol. 9 (1999) 967–970.
[27] H. Nakano, K. Shinohara, Correlation between unirradiated cell TP53 protein levels and radiosensitivity in MOLT-4 cells, Radiat. Res. 151 (1999) 686–693.
[28] A. Enomoto, N. Suzuki, K. Hirano, Y. Matsumoto, A. Morita, K. Sakai, H. Koyama, Involvement of SAPK/JNK pathway in X-ray-induced rapid cell death of human T-cell leukemia cell line MOLT-4, Cancer Lett. 155 (2000) 137–144.
[29] E. Takahashi, O. Inanami, T. Asanuma, M. Kuwabara, Effects of ceramide inhibition on radiation-induced apoptosis in human leukemia MOLT-4 cells, J. Radiat. Res. (Tokyo) 47 (2006) 19–25.
[30] J.F. Weiss, M.R. Landauer, Protection against ionizing radiation by antioxidant nutrients and phytochemicals, Toxicology 189 (2003) 1–20.
[31] N.A. Maianski, D. Roos, T.W. Kuijpers, Tumor necrosis factor alpha induces a caspase-independent death pathway in human neutrophils, Blood 101 (2003) 1987–1995.
[32] M. Okada, S. Adachi, T. Imai, K. Watanabe, S.Y. Toyokuni, M. Ueno, A.S. Zervos, G. Kroemer, T. Nakahata, A novel mechanism for imatinib mesylate-induced cell death of BCR-ABL-positive human leukemic cells: caspase-independent, necrosis-like programmed cell death mediated by serine protease activity, Blood 103 (2004) 2299–2307.
[33] A.S. Cowburn, J.F. White, J. Deighton, S.R. Walmsley, E.R. Chilvers, z-VAD-fmk augmentation of TNF alpha-stimulated neutrophil apoptosis is compound specific and does not involve the generation of reactive oxygen species, Blood 105 (2005) 2970–2972.
[34] A. Kawahara, Y. Ohsawa, H. Matsumura, Y. Uchiyama, S. Nagata, Caspase-independent cell killing by Fas-associated protein with death domain, J. Cell Biol. 143 (1998) 1353–1360.
[35] M. Artal-Sanz, N. Tavernarakis, Proteolytic mechanisms in necrotic cell death and neurodegeneration, FEBS Lett. 579 (2005) 3287–3296.
[36] M.J. Spencer, D.E. Croall, J.G. Tidball, Calpains are activated in necrotic fibers from mdx dystrophic mice, J. Biol. Chem. 270 (1995) 10909–10914.
[37] T. Yamashima, Ca^{2+}-dependent proteases in ischemic neuronal death: a conserved 'calpain–cathepsin cascade' from nematodes to primates, Cell Calcium 36 (2004) 285–293.

Neuroscience 160 (2009) 61–68

MODULATION OF CONNEXIN 43 IN ROTENONE-INDUCED MODEL OF PARKINSON'S DISEASE

A. KAWASAKI,[a,b]* T. HAYASHI,[b] K. NAKACHI,[b] J. E. TROSKO,[c] K. SUGIHARA,[a] Y. KOTAKE[a] AND S. OHTA[a]**

[a]*Graduate School of Biomedical Sciences, Hiroshima University, 1-2-3, Kasumi, Minami-ku, Hiroshima 734–8553, Japan*

[b]*Department of Radiobiology and Molecular Epidemiology, Radiation Effects Research Foundation, 5–2 Hijiyama Park, Minami Ward, Hiroshima, 732–0815, Japan*

[c]*National Food Safety Toxicology Center, Department of Pediatrics/ Human Development, Michigan State University, East Lansing, MI 48824, USA*

Abstract—Gap junctional communication plays an important role in various models of brain pathology, but the changes of gap junctions in Parkinsonism are still not understood. In this study, we show that a major gap junctional protein, connexin43 (Cx43), in astrocytes is enhanced both in a rat Parkinson's disease (PD) model induced with rotenone, a widely used pesticide that inhibits mitochondrial complex I, and *in vitro* in cultured astrocytes stimulated with rotenone. Enhancement of Cx43 protein levels in rotenone-treated cultured astrocytes occurred in parallel with an increase in gap junctional intercellular communication, but was not accompanied with an increase in *Cx43* mRNA levels. Furthermore, the rotenone-induced increase of Cx43 protein levels both *in vitro* and *in vivo* was associated with increased levels of phosphorylated Cx43, which is required for gap junctional intercellular communication. In our rat PD model, phosphorylated Cx43 was selectively enhanced in the basal ganglia regions, which contain DA neurons or their terminal areas. The increase of Cx43 levels was lower in the substantia nigra pars compacta and the striatum than in the substantia nigra pars reticulata and the globus pallidus. Our findings indicate that modulation of Cx43 protein, and consequently gap junctional cellular communication, in astrocytes may play an important role in PD pathology.

Key words: gap junction, connexin 43, astrocyte, Parkinson's disease, dopaminergic, basal ganglia.

Parkinson's disease (PD) is an adult-onset neurodegenerative disease that is characterized by a progressive and fatal loss of dopaminergic (DA) neurons in the substantia nigra and striatum. A prototypical mitochondrial complex inhibitor, 1-methyl-4-phenyl-1,2,3,6-tetrahydropyridine, induces Parkinsonism in humans and other mammals, and systemic administration of another mitochondrial complex I inhibitor, rotenone, also causes selective death of DA neurons and Parkinsonism in rodents, accompanied by behavioral and neurochemical changes, DA degeneration, and the appearance of eosinophilic cytoplasmic inclusions (Betarbet et al., 2000). DA neurons are known to be sensitive to extracellular ions and chemical transmitters, and extracellular K^+ and glutamate were shown to play key roles in DA neuronal cell death in an animal PD model (Obata et al., 2000; Araki et al., 2001; Ransom et al., 2003). The reason why DA neurons are particularly vulnerable to complex I inhibition is not fully understood, although their vulnerability seems to be important in the development of Parkinsonism. In addition, accumulating evidence indicates an active role for nonneuronal cells, specifically astrocytes, in DA neuronal degeneration (Cardona et al., 2006; McGeer and McGeer, 2008). Astrocytes are central to maintaining the homeostatic regulation of extracellular pH, K^+, and glutamate levels (Rouach et al., 2000). However, despite the importance of astrocyte functions, the role of astrocytes in Parkinsonism remains unknown.

We have previously reported that modulation of gap junctional intercellular communication (GJIC) and connexin43 (Cx43) affect cell viability or growth, implying that GJIC may have an important role in maintaining homeostasis in various organs (Hayashi et al., 1997; Ogawa et al., 2005). It has also been reported that GJIC in astrocytes is indispensable for the homeostatic regulation of extracellular pH, K^+, and glutamate levels in the CNS (Anderson and Swanson, 2000; Ransom et al., 2003). Astrocytes are thought to be coupled by gap junctions, which consist of Cx43 (Dermietzel et al., 2000; Nagy and Rash, 2003). Alteration of Cx43 has recently been observed in ischemia, Alzheimer's disease, and Huntington's disease (Nagy et al., 1996; Vis et al., 1998; Kielian, 2008), and an increase or loss of Cx43 and GJIC in astrocytes has been observed after brain injuries and in pathogenesis associated with reactive astrocytosis (Meme et al., 2006; Haupt et al., 2007). However, whether or not altered astrocyte GJIC is involved in the development of PD remains unanswered.

Therefore, in this study we examined the changes in astrocyte GJIC and Cx43, as well as the phosphorylation status of Cx43, in a rat model of PD induced by chronic exposure to rotenone and in cultured astrocytes stimulated with rotenone. The former model has been widely used to investigate the etiology of Parkinsonism (Betarbet et al., 2000; Alam and Schmidt, 2002); the latter is useful to study

*Correspondence to: A. Kawasaki, Graduate School of Biomedical Sciences, Hiroshima University, 1-2-3, Kasumi, Minami-ku, Hiroshima 734-8553, Japan. Tel: +81-82-257-5327.
E-mail address: asamik@hiroshima-u.ac.jp (A. Kawasaki).
**Corresponding author. Tel: +81-82-257-5327.
E-mail address: sohta@hiroshima-u.ac.jp (S. Ohta).

Abbreviations: Cx43, connexin43; DA, dopaminergic; DMSO, dimethyl sulfoxide; FRAP, fluorescence recovery after photobleaching; GJIC, gap junctional intercellular communication; PBST, PBS-0.1% Triton X-100; PD, Parkinson's disease; PVDF, polyvinylidene difluoride; RR, recovery rate; SNc, substantia nigra pars compacta; SNr, substantia nigra pars reticulata; TH, tyrosine hydroxylase.

0306-4522/09 $ - see front matter
doi:10.1016/j.neuroscience.2009.01.080

the molecular mechanisms of rotenone's effects on Cx43 and GJIC.

EXPERIMENTAL PROCEDURES

Drugs and chemicals

Rotenone and dimethyl sulfoxide (DMSO) were purchased from Sigma-Aldrich (St. Louis, MO, USA). Rotenone was dissolved in DMSO (100 mM) and stored at −20 °C.

Rats

The animals were acclimated and maintained at 23 °C under a 12-h light/dark cycle (lights on 08:00–20:00 h). Rats were housed in standard laboratory cages and had free access to food and water throughout the study period. All animal experiments were carried out in accordance with the National Institutes of Health (NIH) Guide for the Care and Use of Laboratory Animals, and the protocols were approved by the Committee for Animal Research at Hiroshima University. All efforts were put in place to minimize the number of animals used and their suffering. Lewis rats (200–250 g each) were purchased from Japan SLC, Inc. (Hamamatsu, Japan). The rats were randomly divided into a rotenone group (n=6) and a control group (n=6). The rotenone group subcutaneously received rotenone (2.5 mg/kg, diluted in Panacet); the controls received vehicle (Panacet) only.

Primary astrocyte cultures

Primary astrocytes were prepared from whole brains of neonatal Wistar rats (1–2 days of age) (Hosoi et al., 2000). In brief, the brains were digested with 0.05% trypsin–EDTA (Invitrogen, Grand Island, NY, USA) at 37 °C for 10 min, and then mechanically dissociated by gentle pipetting and passed through a 70-μm-pore nylon mesh. Cells were plated onto 75 cm^2 plastic flasks and grown in DMEM (Invitrogen) supplemented with 10% v/v heat-inactivated fetal bovine serum (FBS) and 1% penicillin/streptomycin at 37 °C in a humidified 5% CO_2-containing atmosphere. The medium was changed twice a week. When cells reached confluence, at ~12 days *in vitro*, they were harvested with trypsin-EDTA (Invitrogen). Cells were then replated as a secondary culture. The purity of the primary astrocyte cultures was assessed by immunocytochemical staining, using an antibody against an astrocyte-specific marker (GFAP, dilution 1:1000; Sigma-Aldrich). At 30 days *in vitro*, 99% of the primary-cultured cells were GFAP-positive. Cultured astrocytes were treated with 0–16 nM rotenone for 48 h.

Fluorescence recovery after photobleaching (FRAP) assay for GJIC

The procedure used was a modified version of the standard method for measuring GJIC by quantitative FRAP (Wade et al., 1986; Trosko et al., 2000). Assays were performed using a Zeiss LSM 510 laser-scanning confocal microscope (Carl Zeiss International, Jena, Germany). After bleaching of randomly selected cells with a micro-laser beam, the rate of transfer of 5,6-carboxyfluorescein diacetate (Molecular Probes, Inc., Eugene, OR, USA) from adjacent labeled cells back into bleached cells was calculated. Recovery of fluorescence was examined after 0.5 min, and the recovery rate (RR) was calculated as percentage of photobleached fluorescence per min. The RR was adjusted for the loss of fluorescence measured in unbleached cells, and the results are expressed as the ratio (mean±SE) of RR to that of untreated control cells.

Extraction of Cx43 RNA

Cells were grown in 6-cm dishes and prepared as described previously (Ogawa et al., 2005). In brief, after 48 h of incubation, the cells were trypsinized and suspended in DMEM medium containing 10% FCS. Total RNA was isolated from the cells using QIAshredder and RNeasy Mini kits (Qiagen, Inc., Chatsworth, CA, USA). An initial strand of cDNA was synthesized from 500 ng of RNA extracts in a volume of 20 μl using AMV reverse transcriptase XL (TaKaRa, Otsu, Japan) priming with random 9-mers at 42 °C for 10 min. The cDNA strand was stored at −20 °C until use. Expression of *rCx43* mRNAs was evaluated by real-time RT PCR based on TaqMan methodology. In brief, PCR was performed in an ABI PRISM 7900 sequence detector (PerkinElmer/Applied Biosystems, Foster City, CA, USA) in a final volume of 20 μl. The PCR mixture contained 10 mM Tris–HCl buffer, pH 8.3 (PerkinElmer/Applied Biosystems), 50 mM KCl, 1.5 mM $MgCl_2$, 0.2 mM dNTP mixture, 0.5 U of "AmpliTaq Gold" (PerkinElmer/Applied Biosystems), 0.2 μM primers and probe. The primer and probe sequences for gene amplification were as follows: rCx43; 5-ATCAGCATCCT CTTCAAGTCTGTCT-3 (FP), 5-CAGGGA-TCTCTCTTGCA−GGTGTA-3 (RP) and 5-CC TGCTCATCCAGT-GGT-3 (probe). The "TaqMan" probe carried a 5-FAM reporter label and a 3-MGB and nonfluorescence quencher group, synthesized by Applied Biosystems. The determination of *rGAPDH* used the TaqMan rodent GAPDH control reagents (Applied Biosystems). The AmpliTaq gold enzyme was activated by heating for 10 min at 95 °C, and all genes were amplified by 50 cycles of heating for 15 s at 95 °C, followed by 1 min at 60 °C.

Quantification for *Cx43* mRNA

For the construction of standard curves of positive controls, the total RNA of primary astrocytes was reverse-transcribed into cDNA and serially diluted in water in five or six log steps to afford fourfold serial dilutions of cDNA from about 100 ng to 100 pg. These cDNA serial dilutions were prepared once for all examinations performed in this study and stored at −20 °C. The coefficient of linear regression for each standard curve was calculated, and then when the cycle threshold (CT) value of a sample was substituted in the formula for each standard curve, the relative concentration of *rCx43* or *rGAPDH* could be calculated. To normalize for differences in the amount of total RNA added to each reaction mixture, *GAPDH* was used as an endogenous RNA control. The data represent the average expression of target genes, relative to *GAPDH*, from three independent cultures.

Immunoblotting

Cells and rat brains were lysed in ice-cold lysis buffer containing 20 mM Tris-buffered saline (TBS), pH 7.5, 1% Triton X-100, 150 mM NaCl, and 1 mM each of EDTA, EGTA, β-glycerophosphate, Na_3VO_4, and phenylmethylsulfonyl fluoride, 2.5 mM sodium pyrophosphate, 1 μg/ml leupeptin. The lysates were then sonicated. The samples were diluted 1:4 in water, and their protein concentrations were determined using DC protein assay (Bio-Rad Corp., Richmond, CA, USA). Samples (10 μg) of protein were dissolved in Laemmli Sample Buffer, separated on 12.5% acrylamide gel, and transferred to polyvinylidene difluoride (PVDF) membranes (Bio-Rad). Then blots were incubated with anti-Cx43 monoclonal antibody (Chemicon International, Inc., Temecula, CA, USA) overnight at 4 °C, followed by PBS-0.1% Triton X-100 (PBST) washes three times for 15 min each. As an internal control to determine whether equal amounts of protein had been loaded on to the gel, the PVDF membranes were stripped and reprobed with anti-α-tubulin (T5168, Sigma-Aldrich). Blots were incubated with goat–antirabbit antibody–conjugated horseradish peroxidase or mouse–antimouse antibody–conjugated horseradish peroxidase. Immunoreactivity was determined by ECL detection using the ECL

plus (GE Healthcare, Piscataway, NJ, USA) according to the manufacturer's instruction.

Immunochemical staining

Antibodies against total Cx43 and phosphorylated Cx43 were used. Cells or brain sections were fixed with 4% paraformaldehyde plus 15% sucrose in PBS, pH 7.4, at room temperature for 30 min and then permeabilized with 0.1% Triton X-100 at room temperature for an additional 30 min. Nonspecific antibody binding was blocked by incubating cells with 5% bovine serum albumin (BSA) in PBS for 1 h at room temperature. Slides were incubated overnight at 4 °C with anti-Cx43 monoclonal antibody (Chemicon) at 1:500 dilution, anti-phospho-Cx43 polyclonal antibody (Cell Signaling) at 1:500 dilution, anti-GFAP antibody at 1:1000 dilution (Sigma-Aldrich), or anti–tyrosine hydroxylase (TH) polyclonal antibody (Chemicon) at 10,000 dilution. Next, the cells were washed three times with PBST and incubated with Alexa 546–conjugated goat antimouse antibody and Alexa 488–conjugated goat antirabbit antibody (Molecular Probes) at a dilution of 1:500 overnight at 4 °C, in the dark. The slides were then washed three times in PBST and once in PBS prior to being mounted in ProLong gold Antifade Reagent (Invitrogen). Finally the cells were examined using a Zeiss LSM 510 laser-scanning confocal microscope (Carl Zeiss International). Negative control, mouse or rabbit IgG was substituted for the primary antibodies.

Statistical analysis

Data were analyzed using SPSS software (version 16). The two-tailed unpaired *t*-test was used to determine the significance of mean differences between two groups.

RESULTS

Rotenone enhanced total Cx43 protein level of cultured astrocytes

Western blotting was carried out to determine whether the GJIC activity of astrocytes was related to total Cx43 protein level and/or to the extent of Cx43 phosphorylation. Three forms of Cx43 immunoreactive protein (Mr 41,000–43,000) were observed in all samples: A faster migrating band (non-phosphorylated form, P_0) and two slower migrating adjacent bands (two phosphorylated forms, P_1 and P_2; Fig. 1A). Densitometric analysis showed that rotenone induced a significant dose- and time-dependent increase of $P_0+P_1+P_2$ (total Cx43) compared with control cells (Fig. 1A, fold increase) over 6–48 h (Fig. 1A, lower panel). The effect of rotenone on *Cx43* mRNA levels was also examined, and *Cx43* mRNA levels were found not to be changed by rotenone treatment (Fig. 2).Next, we examined Cx43 localization in astrocytes, since phosphorylated Cx43, P_1 and P_2, are known to localize on the plasma membrane and gap junctions. The localization and protein levels of total Cx43 and phosphorylated Cx43 were then examined by indirect immunofluorescence cytochemistry. Fig. 1B shows immunostaining for total Cx43 (red) and phosphorylated Cx43 (green) after 48 h treatment with or without rotenone (a–d: control, a′–d′: rotenone). In control cells, total Cx43 immunoreactivity was scattered throughout the cytosol and on the plasma membrane (Fig. 1Ba), while rotenone treatment caused an increase in the distribution area and protein level of total Cx43, and the cells displayed marked linear or intermittent labeling, apparently

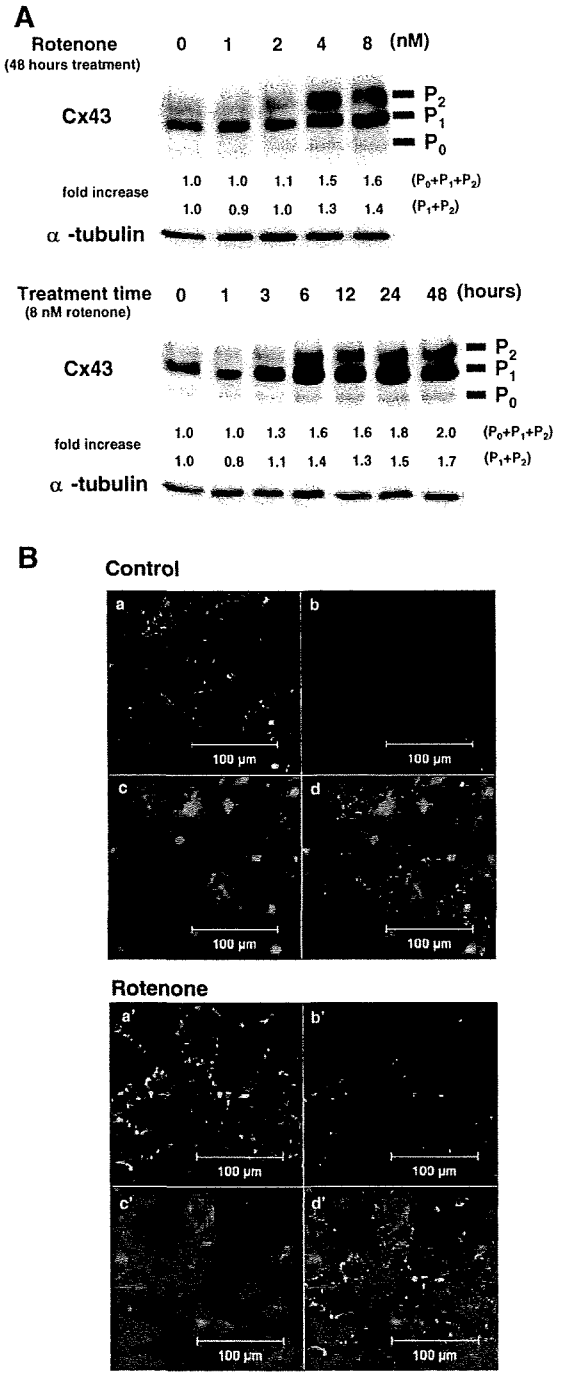

Fig. 1. Effects of rotenone on Cx43 levels. (A) Western blot analysis of Cx43 protein expression. Astrocytes were cultured with or without rotenone for 48 h at the indicated concentrations (upper panel) or with 8 nM rotenone for the indicated times (lower panel). Fold increase after culturing with rotenone is shown taking the value of untreated astrocytes as unity. (B) Intracellular localization of total Cx43 and phosphorylated Cx43 with or without 8 nM rotenone treatment for 48 h. Phosphorylated Cx43 was stained green with FITC (a, a′), and Cx43 was stained red with Cy3 (b, b′). GFAP was stained blue with Alexa 405 (c, c′). The merged image is yellow at areas of colocalization (d, d′). Images were acquired using confocal microscopy. Scale bars=100 μm.

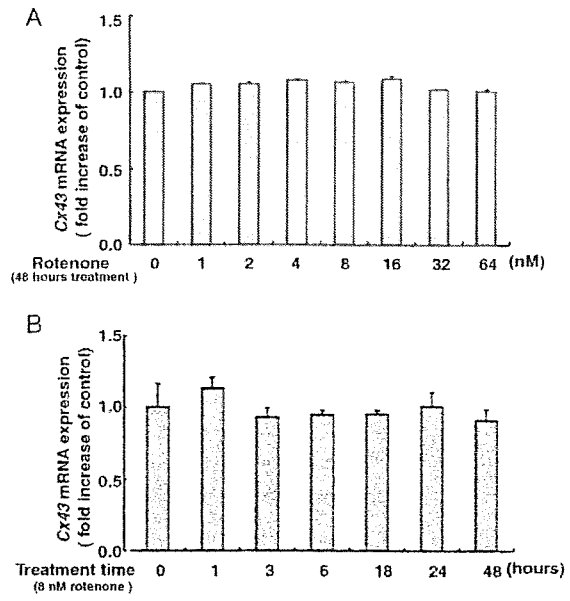

Fig. 2. Real-time RT-PCR analysis of *Cx43* mRNA expression. Astrocytes were cultured with or without rotenone for 48 h at the indicated concentrations (A) or with 8 nM rotenone for the indicated times (B). The value of untreated astrocytes (control) was taken as unity to calculate the fold increase. *Cx43* mRNA levels were normalized by *GAPDH* mRNA, whose level did not change during culture with rotenone (data not shown). Results are means of at least three experiments. Values are mean±SE.

along the plasma membrane between cells (Fig. 1Ba′). Enhanced total Cx43 foci were co-localized with phosphorylated Cx43 (Fig. 1Bd′) in the rotenone-treated cells. These results suggest that upregulation and trafficking of Cx43 protein to the membrane were induced by rotenone.

Rotenone enhanced GJIC through Cx43 in cultured astrocytes

We next examined the effect of rotenone on GJIC in cultured astrocytes. The GJIC was assessed by the FRAP technique, in terms of the RR. After photobleaching, sequential scans detected the recovery of fluorescence in the bleached cells as the dye was transferred to photobleached cells through GJIC from surrounding non-bleached cells. The RR at 48 h of treatment showed a dose-dependent increase up to 8 nM rotenone, although this was followed by a slight decrease (Fig. 3A). Further, time course analysis showed a time-dependent increase in GJIC after rotenone treatment (Fig. 3B). These results suggest that rotenone treatment of cultured astrocytes generated increased protein levels and a broadened membrane distribution of Cx43, which in turn led to enhancement of GJIC.

Total and phosphorylated Cx43 protein levels were enhanced in astrocytes in the rat PD model

To investigate whether Cx43 levels may be altered in Parkinsonism, we examined the Cx43 protein level and immunoreactivity in our rotenone-induced rat PD model. In this model, chronic exposure to rotenone remarkably reduced TH immunoreactivity in the substantia nigra pars compacta (SNc), the same area where loss of DA neurons occurs in human PD (Supplementary Fig. 1). Fig. 6 shows that Cx43 was found in all regions, though at different levels, and that the Cx43 protein level was significantly lower in striatum than in other brain regions (Fig. 4), though the P_1 and P_2 forms of Cx43 were markedly enhanced in striatum of the treated group. Significant differences of total Cx43 levels were found in striatum of rotenone-treated rats at 1, 2, and 4 weeks, as well as in hippocampus of rotenone-treated rats at 1 week. However, no significant changes were observed in other regions (Fig. 5A, B). Next, Cx43 immunohistochemistry was performed on the SN and striatum and globus pallidus (GP) of vehicle- or rotenone-treated rats (Fig. 6). In the SN, Cx43 immunoreactivity was enhanced in rotenone-treated rats compared with that in vehicle-treated rats. Elevation of Cx43 was more noticeable in substantia nigra pars reticulata (SNr) than in SNc (Fig. 6A). Increase of Cx43 after rotenone treatment was more pronounced in GP than striatum (Fig. 6B).

SNc and striatum in rotenone-treated rats revealed DA neuronal loss when visualized by TH immunoreactivity (Fig. 6), consistent with previous observations (Betarbet et al., 2000). Interestingly, the degree of enhancement of Cx43 by rotenone was found to be lower in SNc and striatum than in other regions (Fig. 6, Cx43).

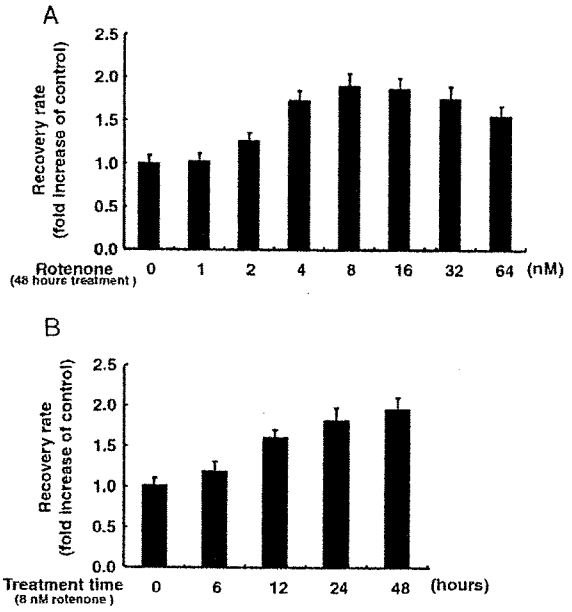

Fig. 3. Dose and time course analyses of the effect of rotenone on GJIC in cultured astrocytes. GJIC was assessed by FRAP, in terms of RR (fold increase of control cells). Results are means of at least three experiments. (A) Dose dependence (treatment for 48 h). (B) Time dependence in the case of 8 nM rotenone. Columns show fold increase in RR compared with untreated cells (at 48 h) or compared with cells treated with 8 nM rotenone at 0 h for A or B, respectively. $P_{trend}<0.001$ for A and B.

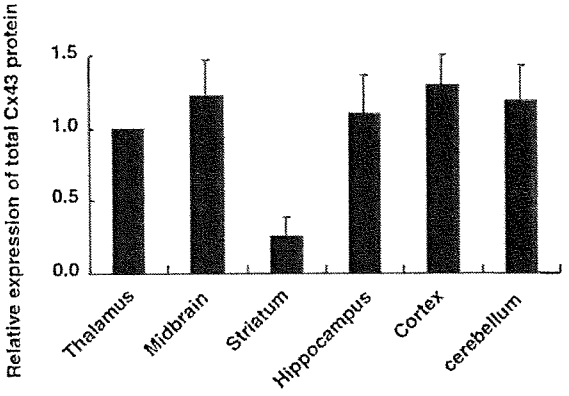

Fig. 4. Cx43 levels were compared between different brain regions by using identical membranes loaded with the homogenates obtained from the different regions. The graph depicts fold increase of total Cx43 expression relative to the control (thalamus). Values are mean±SE with $n=3$.

In addition, although astrocytes were denser in SNr and GP than in SNc and striatum, the numbers of astrocytes in nigrostriatal regions was unchanged with rotenone treatment (Fig. 6, GFAP).

DISCUSSION

Previous Cx43 electrophoresis studies had found a faster-migrating form that includes nonphosphorylated Cx43 (P_0) and at least two slower-migrating forms, commonly termed P_1 and P_2 (Crow et al., 1990; Musil et al., 1990). Pulse-chase analysis had indicated that the Cx43 isoforms progress from P_0 to P_1 to P_2 and that the P_2 isoform is associated with gap junctional structures (Musil and Goodenough, 1991). In our study, rotenone treatment induced an increase of total Cx43 protein in astrocytes, and the number of localized foci of total and phosphorylated Cx43 on the plasma membrane was increased. Furthermore, astrocyte GJIC was intensified with rotenone treatment. Therefore, since the increase of P_1 and P_2forms of Cx43 was proportional to the increase of total Cx43 protein levels, our findings indicate that phosphorylation of P_0 and P_1 was enhanced during the induction of total Cx43 protein by rotenone. Cowan et al. (2003) reported that Cx43 protein levels decreased in response to rotenone treatment, but their finding cannot be directly compared with ours, since they used vascular smooth muscle cells and a far higher concentration (10 μM) of rotenone.

On the other hand, since *Cx43* mRNA levels did not change, altered protein degradation may be involved in the rotenone-induced increase of Cx43 protein. Degradation of Cx43 is thought to be regulated by phosphorylation of P_0, or possibly P_1 and P_2 (Rivedal and Opsahl, 2001; Ruch et al., 2001; Qin et al., 2003). Phosphorylation is implicated in the regulation of GJIC at several stages of the connexin "life cycle," including trafficking, assembly/disassembly, and gating of gap junction channels (Lampe and Lau, 2004). Our *in vivo* experiment using rotenone-treated rats demonstrated for the first time that P_1 and P_2 forms of Cx43 are selectively induced in astrocytes of the basal ganglia regions, which contain DA neurons or their terminal areas, and that these elevated levels of Cx43 were sustained during rotenone treatment. This site-specific

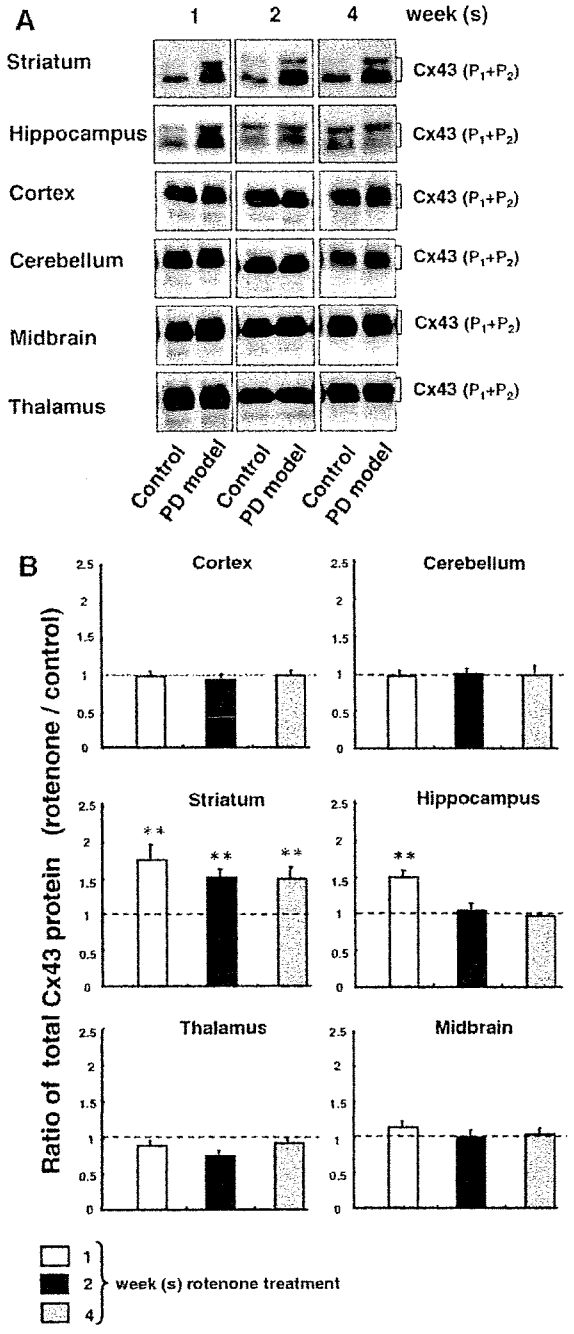

Fig. 5. Cx43 levels in the brain of rotenone-treated rats relative to that of Panacet (vehicle)-treated rats (control) at 1, 2, and 4 weeks. (A) Western blotting analysis of Cx43. (B) Column illustrates the quantifications of Cx43 levels obtained from three independent experiments by measuring the intensity of the Cx43 signal. Values are mean±SE with $n=6$. ** $P<0.05$ for the mean difference from the corresponding control group.

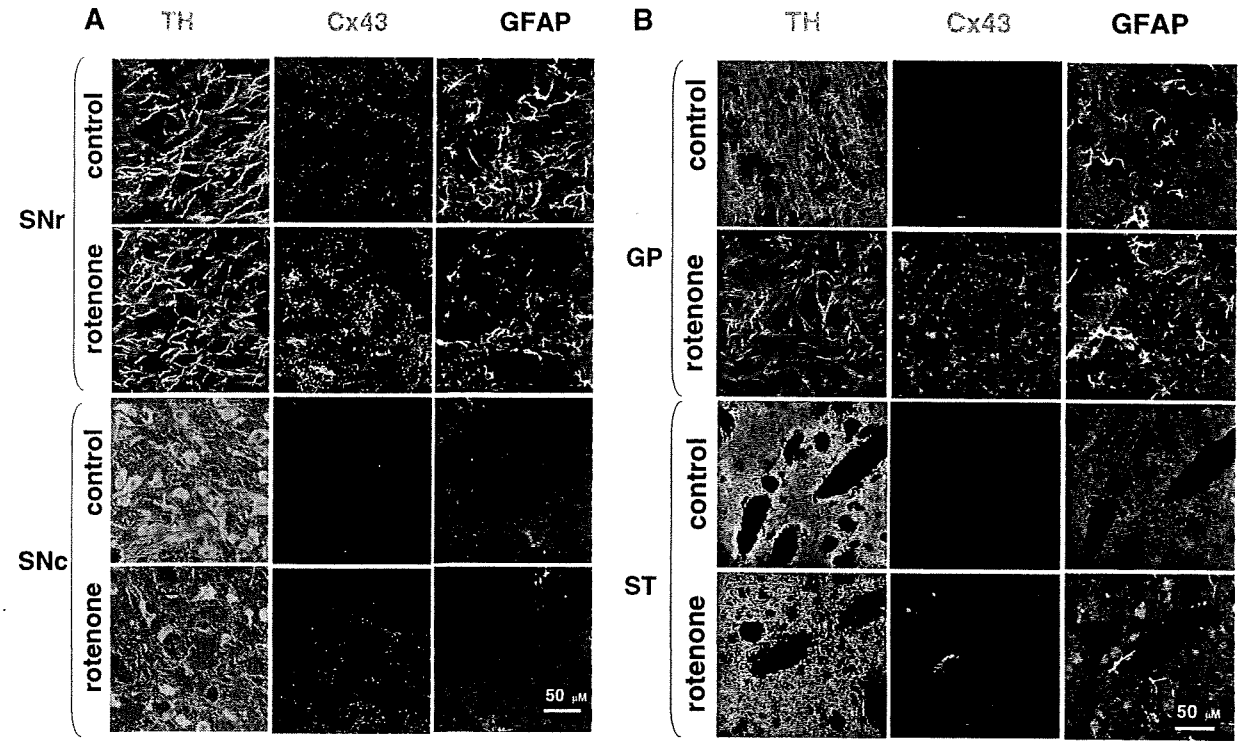

Fig. 6. Immunofluorescence staining of (A) SN and (B) ST obtained from Panacet- (vehicle) or rotenone-treated rat brain at 4 weeks. Triple labeling was used, with TH colored green, Cx43 colored red, and GFAP, an astrocyte marker, colored white. In (B) GP or ST indicates globus pallidus or striatum, respectively. Scale bars=50 μM.

susceptibility of astrocytes to Cx43 induction by rotenone could be of great importance, since the great heterogeneity of astrocytes among brain sites is a key to understanding PD pathology (Price et al., 1999; Amadio et al., 2007).

This study has obvious limitations, and some tasks for future investigation are mentioned below. Although induction of astrocyte Cx43 by rotenone was observed along with loss of DA neurons in the SNc and striatum, we failed to establish a relationship between increase of Cx43 and extent of DA neuron damage: induced levels of Cx43 were lower in SNc and striatum than in SNr and GP, though DA neurons in the SNc and striatum are more vulnerable than those in SNr and GP (Fearnley and Lees, 1991). Further study will be necessary to assess the site-specific vulnerability of DA neurons in the nigrostriatal area, and the potential involvement of mechanisms, such as inflammation, other than GJIC in the selective death of DA neurons. Induction of Parkinsonism by rotenone will need to be examined. For example, the inflammation that is thought to cause activation of astrocytes, which is in turn associated with upregulation of Cx43, may involve microglia (Retamal et al., 2007). In addition, Cx30 and Cx26 are both major gap junction proteins in astrocytes. We found that Cx26 expression was unaffected by rotenone *in vivo* and *in vitro* (data not shown), but it will also be necessary to examine changes in Cx30 in the future, perhaps with the use of Cx.-specific inhibitors or siRNA.

The central question is whether the elevation of astrocyte GJIC plays a part in causing the development of PD or whether it is merely a protective response to rotenone. Astrocytic syncytia in the normal CNS play important homeostatic roles in the spatial buffering of extracellular potassium ions and water (Jefferys, 1995; Naus et al., 1997; Wallraff et al., 2006), glutamate and other signaling molecules (Cornell-Bell et al., 1990; Hossain et al., 1994), and energy sources (Dienel and Cruz, 2003). On the other hand, abnormal synchronization of the oscillatory activity of neurons at multiple levels of the basal ganglia–cortical loop is thought to play a role in this synchronization in animal models and human PD. This suggests the possibility that enhancement of GJIC affects PD development (Yamawaki et al., 2008). To examine whether this is so, the effects of astrocyte GJIC inhibition on DA neurons in PD models needs to be investigated using an astrocyte-specific GJIC inhibitor; however, such an inhibitor is not yet available. Cx. knockout mice might be useful to investigate the role of gap junctions in PD models. Furthermore, it is of interest to know why the change of Cx43 occurred in the hippocampus. Our immunohistological analysis suggested that the number of astrocytes in striatum and hippocampus is higher than those in other brain regions. Therefore one possibility is that this difference in the density of astrocytes influences the induction of Cx43 protein by rotenone. Another possibility is that astrocytes in striatum and hip-

pocampus might have different characteristics from those in other areas (Price et al., 1999; Amadio et al., 2007).

Rufer et al. (1996) reported that immunoreactive Cx43 protein was increased in the striatum in a rat MPTP model, but they did not find evidence of increased functional coupling. They did not examine cultured astrocytes. The reason for the difference between their results and ours is unclear, but may be related to the differences between the rotenone and MPTP models. In summary, rotenone enhanced GJIC through induction of phosphorylated Cx43 as well as total Cx43 in astrocytes, and increased Cx43 in nigrostriatal astrocytes was also observed in rotenone-treated rats, accompanied with loss of DA neurons. Given the potential implications of our findings, the mechanisms linking enhanced astrocyte GJIC and DA neuron death urgently need to be examined.

Acknowledgments—The authors would like to thank Dr. Takashi Taniguchi and Dr. Yoshihisa Kitamura and Takashi Yanagida from Kyoto Pharmaceutical University, and Dr. Koichiro Ozawa and Dr. Toru Hosoi from Graduate School of Biomedical Sciences, Hiroshima University.

REFERENCES

Alam M, Schmidt WJ (2002) Rotenone destroys dopaminergic neurons and induces parkinsonian symptoms in rats. Behav Brain Res 136:317–324.

Amadio S, Montilli C, Picconi B, Calabresi P, Volonte C (2007) Mapping P2X and P2Y receptor proteins in striatum and substantia nigra: an immunohistological study. Purinergic Signal 3:389–398.

Anderson CM, Swanson RA (2000) Astrocyte glutamate transport: review of properties, regulation, and physiological functions. Glia 32:1–14.

Araki T, Kumagai T, Tanaka K, Matsubara M, Kato H, Itoyama Y, Imai Y (2001) Neuroprotective effect of riluzole in MPTP-treated mice. Brain Res 918:176–181.

Betarbet R, Sherer TB, MacKenzie G, Garcia-Osuna M, Panov AV, Greenamyre JT (2000) Chronic systemic pesticide exposure reproduces features of Parkinson's disease. Nat Neurosci 3:1301–1306.

Cardona AE, Pioro EP, Sasse ME, Kostenko V, Cardona SM, Dijkstra IM, Huang D, Kidd G, Dombrowski S, Dutta R, Lee JC, Cook DN, Jung S, Lira SA, Littman DR, Ransohoff RM (2006) Control of microglial neurotoxicity by the fractalkine receptor. Nat Neurosci 9:917–924.

Cornell-Bell AH, Finkbeiner SM, Cooper MS, Smith SJ (1990) Glutamate induces calcium waves in cultured astrocytes: long-range glial signaling. Science 247:470–473.

Cowan DB, Jones M, Garcia LM, Noria S, del Nido PJ, McGowan FX Jr (2003) Hypoxia and stretch regulate intercellular communication in vascular smooth muscle cells through reactive oxygen species formation. Arterioscler Thromb Vasc Biol 23:1754–1760.

Crow DS, Beyer EC, Paul DL, Kobe SS, Lau AF (1990) Phosphorylation of connexin43 Gap junction protein in uninfected and Rous sarcoma virus-transformed mammalian fibroblasts. Mol Cell Biol 10:1754–1763.

Dermietzel R, Gao Y, Scemes E, Vieira D, Urban M, Kremer M, Bennett MV, Spray DC (2000) Connexin 43 null mice reveal that astrocytes express multiple connexins. Brain Res Brain Res Rev 32:45–56.

Dienel GA, Cruz NF (2003) Neighborly interactions of metabolically-activated astrocytes in vivo. Neurochem Int 43:339–354.

Fearnley JM, Lees AJ (1991) Ageing and Parkinson's disease: substantia nigra regional selectivity. Brain 114(5):2283–2301.

Haupt C, Witte OW, Frahm C (2007) Upregulation of connexin 43 in the glial scar following photothrombotic ischemic injury. Mol Cell Neurosci 35:89–99.

Hayashi T, Matesic DF, Nomata K, Kang KS, Chang CC, Trosko JE (1997) Stimulation of cell proliferation and inhibition of gap junctional intercellular communication by linoleic acid. Cancer Lett 112:103–111.

Hosoi T, Okuma Y, Nomura Y (2000) Expression of leptin receptors and induction of IL-1beta transcript in glial cells. Biochem Biophys Res Commun 273:312–315.

Hossain MZ, Peeling J, Sutherland GR, Hertzberg EL, Nagy JI (1994) Ischemia-induced cellular redistribution of the astrocytic gap junctional protein connexin43 in rat brain. Brain Res 652:311–322.

Jefferys JG (1995) Nonsynaptic modulation of neuronal activity in the brain: electric currents and extracellular ions. Physiol Rev 75: 689–723.

Kielian T (2008) Glial connexins and gap junctions in CNS inflammation and disease. J Neurochem 106:1000–1016.

Lampe PD, Lau AF (2004) The effects of connexin phosphorylation on gap junctional communication. Int J Biochem Cell Biol 36:1171–1186.

McGeer PL, McGeer EG (2008) Glial reactions in Parkinson's disease. Mov Disord 23:474–483.

Meme W, Calvo CF, Froger N, Ezan P, Amigou E, Koulakoff A, Giaume C (2006) Proinflammatory cytokines released from microglia inhibit gap junctions in astrocytes: potentiation by beta-amyloid. FASEB J 20:494–496.

Musil LS, Cunningham BA, Edelman GM, Goodenough DA (1990) Differential phosphorylation of the Gap junction protein connexin43 in junctional communication-competent and -deficient cell lines. J Cell Biol 111:2077–2088.

Musil LS, Goodenough DA (1991) Biochemical analysis of connexin43 intracellular transport, phosphorylation, and assembly into gap junctional plaques. J Cell Biol 115:1357–1374.

Nagy JI, Li W, Hertzberg EL, Marotta CA (1996) Elevated connexin43 immunoreactivity at sites of amyloid plaques in Alzheimer's disease. Brain Res 717:173–178.

Nagy JI, Rash JE (2003) Astrocyte and oligodendrocyte connexins of the glial syncytium in relation to astrocyte anatomical domains and spatial buffering. Cell Commun Adhes 10:401–406.

Naus CC, Bechberger JF, Zhang Y, Venance L, Yamasaki H, Juneja SC, Kidder GM, Giaume C (1997) Altered gap junctional communication, intercellular signaling, and growth in cultured astrocytes deficient in connexin43. J Neurosci Res 49:528–540.

Obata T, Aomine M, Yamanaka Y (2000) Potassium chloride depolarization enhances MPP+-induced hydroxyl radical generation in the rat striatum. Brain Res 852:488–491.

Ogawa T, Hayashi T, Tokunou M, Nakachi K, Trosko JE, Chang CC, Yorioka N (2005) Suberoylanilide hydroxamic acid enhances gap junctional intercellular communication via acetylation of histone containing connexin 43 gene locus. Cancer Res 65:9771–9778.

Price CJ, Kim P, Raymond LA (1999) D1 dopamine receptor-induced cyclic AMP-dependent protein kinase phosphorylation and potentiation of striatal glutamate receptors. J Neurochem 73:2441–2446.

Qin H, Shao Q, Igdoura SA, Alaoui-Jamali MA, Laird DW (2003) Lysosomal and proteasomal degradation play distinct roles in the life cycle of Cx43 in gap junctional intercellular communication-deficient and -competent breast tumor cells. J Biol Chem 278: 30005–30014.

Ransom B, Behar T, Nedergaard M (2003) New roles for astrocytes (stars at last). Trends Neurosci 26:520–522.

Retamal MA, Froger N, Palacios-Prado N, Ezan P, Saez PJ, Saez JC, Giaume C (2007) Cx43 hemichannels and gap junction channels in astrocytes are regulated oppositely by proinflammatory cytokines released from activated microglia. J Neurosci 27:13781–13792.

Rivedal E, Opsahl H (2001) Role of PKC and MAP kinase in EGF- and TPA-induced connexin43 phosphorylation and inhibition of gap

junction intercellular communication in rat liver epithelial cells. Carcinogenesis 22:1543–1550.

Rouach N, Glowinski J, Giaume C (2000) Activity-dependent neuronal control of gap-junctional communication in astrocytes. J Cell Biol 149:1513–1526.

Ruch RJ, Trosko JE, Madhukar BV (2001) Inhibition of connexin43 gap junctional intercellular communication by TPA requires ERK activation. J Cell Biochem 83:163–169.

Rufer M, Wirth SB, Hofer A, Dermietzel R, Pastor A, Kettenmann H, Unsicker K (1996) Regulation of connexin 43, GFAP, and FGF-2 is not accompanied by changes in astroglial coupling in MPTP-lesioned, FGF-2-treated parkinsonian mice. J Neurosci Res 46:606–617.

Trosko JE, Chang CC, Wilson MR, Upham B, Hayashi T, Wade M (2000) Gap junctions and the regulation of cellular functions of stem cells during development and differentiation. Methods 20:245–264.

Vis JC, Nicholson LF, Faull RL, Evans WH, Severs NJ, Green CR (1998) Connexin expression in Huntington's diseased human brain. Cell Biol Int 22:837–847.

Wade MH, Trosko JE, Schindler M (1986) A fluorescence photobleaching assay of gap junction-mediated communication between human cells. Science 232:525–528.

Wallraff A, Kohling R, Heinemann U, Theis M, Willecke K, Steinhauser C (2006) The impact of astrocytic gap junctional coupling on potassium buffering in the hippocampus. J Neurosci 26: 5438–5447.

Yamawaki N, Stanford IM, Hall SD, Woodhall GL (2008) Pharmacologically induced and stimulus evoked rhythmic neuronal oscillatory activity in the primary motor cortex in vitro. Neuroscience 151:386–395.

APPENDIX

Supplementary data

Supplementary data associated with this article can be found, in the online version, at doi: 10.1016/j.neuroscience.2009.01.080.

(Accepted 31 January 2009)
(Available online 13 February 2009)

Int. J. Radiat. Biol., Vol. 86, No. 1, January 2010, pp. 56–62

informa
healthcare

Memory CD4 T-cell subsets discriminated by CD43 expression level in A-bomb survivors

SEISHI KYOIZUMI[1,3], MIKA YAMAOKA[1], YOSHIKO KUBO[1], KANYA HAMASAKI[1], TOMONORI HAYASHI[1], KEI NAKACHI[1], FUMIYOSHI KASAGI[2], & YOICHIRO KUSUNOKI[1]

Departments of [1]Radiobiology/Molecular Epidemiology and [2]Epidemiology, Radiation Effects Research Foundation, and [3]Department of Nutritional Sciences, Faculty of Human Ecology, Yasuda Women's University, Hiroshima, Japan

(Received 27 October 2008; Revised 18 May 2009; Accepted 20 July 2009)

Abstract

Purpose: Our previous study showed that radiation exposure reduced the diversity of repertoires of memory thymus-derived cells (T cells) with cluster of differentiation (CD)- 4 among atomic-bomb (A-bomb) survivors. To evaluate the maintenance of T-cell memory within A-bomb survivors 60 years after radiation exposure, we examined functionally distinct memory CD4 T-cell subsets in the peripheral blood lymphocytes of the survivors.

Methods: Three functionally different subsets of memory CD4 T cells were identified by differential CD43 expression levels and measured using flow cytometry. These subsets consist of functionally mature memory cells, cells weakly responsive to antigenic stimulation, and those cells functionally anergic and prone to spontaneous apoptosis.

Results: The percentages of these subsets within the peripheral blood CD4 T-cell pool all significantly increased with age. Percentages of functionally weak and anergic subsets were also found to increase with radiation dose, fitting to a log linear model. Within the memory CD4 T-cell pool, however, there was an inverse association between radiation dose and the percentage of functionally mature memory cells.

Conclusion: These results suggest that the steady state of T cell memory, which is regulated by cell activation and/or cell survival processes in subsets, may have been perturbed by prior radiation exposure among A-bomb survivors.

Keywords: *A-bomb, CD4, immunological memory, CD43, flow cytometry, T cell*

Introduction

In humans, immunological memory resides in and is controlled by long-lived lymphocytes, with immunologic memory being maintained at an appropriate level by a constant proliferation of memory thymus-derived cells (T cells) (Dutton et al. 1998). Once subjected to antigenic stimulation, memory T cells tend to divide repeatedly, thus giving rise to greatly expanded clonal populations which may persist for very long periods of time (Maini et al. 1999). Clonally expanded T-cell populations are frequently observed not only in healthy aged persons (Posnett et al. 1994, Fitzgerald et al. 1995, Wack et al. 1998) but also in virally-infected individuals (Eiraku et al. 1998, Silins et al. 1998) and in patients with autoimmune diseases of various types (Fitzgerald et al. 1995, Musette et al. 1996, Waase et al. 1996).

In general, the peripheral blood pool of memory T cells with cluster of differentiation (CD)- 4 appear not to have been significantly affected by radiation exposure among atomic-bomb (A-bomb) survivors. However, there are significant dose-dependent deficits in the naïve T-cell pools (Kusunoki et al. 1998, 2002, Yamaoka et al. 2004). Further, clonal populations originating from peripheral T cells have been identified in blood samples from some of the A-bomb survivors primarily by tracking specific T-cell receptor (TCR) genes and/or chromosome aberrations in memory T-cell populations (Kusunoki et al. 1993, Nakano et al. 2004). In this regard, we have recently reported that the extent of deviation in the TCR repertoire of memory CD4 T cells significantly increased as the intensity of radiation exposure increased (Kusunoki et al. 2003). It seems reasonable, therefore, to assume that A-bomb radiation

Correspondence: Yoichiro Kusunoki, PhD, Department of Radiobiology/Molecular Epidemiology, Radiation Effects Research Foundation, 5-2 Hijiyama Park, Minami-ku, Hiroshima, 732-0815 Japan. Tel: +81 82261 3131. Fax: +81 82261 3170. E-mail: ykusunok@rerf.or.jp

ISSN 0955-3002 print/ISSN 1362-3095 online © 2010 Informa UK Ltd.
DOI: 10.3109/09553000903272641

induced the expansion or shrinkage of particular memory T-cell clones, concomitant with a reduced capacity to maintain fully diverse repertoires of helper T-cell memory.

Previously, we have reported that human memory CD4 T cells can be discriminated into three functionally different subsets (M1, M2, and M3) using the human stem cell-associated (HSCA)- 2 monoclonal antibody (mAb) that recognises a sialic acid-dependent epitope on the low molecular mass (~ 115 kDa) glycoform of CD43 (Ohara et al. 2002, Kyoizumi et al. 2004). The M1 subset consists of functionally mature cells whose CD43 expression is relatively high. The M2 subset expresses moderate levels of CD43, and responds weakly to TCR-mediated stimuli. The M3 subset exhibits relatively low levels of CD43 and is anergic to TCR-mediated stimuli, and prone to spontaneous apoptosis.

In this study, we evaluated the extent to which T-cell memory function is retained in A-bomb survivors by examining the relationships between these memory CD4 T-cell subsets, ageing, and radiation exposure.

Materials and methods

Blood donors

An A-bomb survivor cohort was randomly selected from a group of Hiroshima participants in the Adult Health Study (AHS) at the Radiation Effects Research Foundation (RERF) (Kodama et al. 1996).

For the present study, blood samples of 1132 survivors were obtained, with informed consent, from survivors who participated in the AHS between 2004 and 2008. This study protocol has been approved by the Human Investigation Committee of RERF. We excluded 216 subjects (19% in total subjects) who had been diagnosed with cancer from the current study. Cancer prevalence by dose category was 16% at <0.005 Gy, 21% at 0.005–0.5 Gy, 30% at 0.5–1.0 Gy, and 35% at ≥1.0 Gy, and tended to be higher in survivors exposed to higher doses, in accord with a recent observation in the AHS population (Kyoizumi et al. 2005). The age, gender and radiation dose of the remaining 916 survivors whose lymphocyte samples were subjected to data analysis in our study are listed in Table I. Radiation doses are based on the Dosimetry System 2002 (DS02) estimates (Cullings et al. 2006).

Table I. Age, gender, and radiation dose distribution of study population.

Dose (Gy)	Age (yrs)[b] category						
	60–69 yrs		70–79 yrs		≥80 yrs		
	Male	Female	Male	Female	Male	Female	Total
<0.005[a]	27	25	58	84	17	94	305
0.005–0.5	13	33	54	66	22	107	295
0.5–1.0	19	18	20	33	9	49	148
1.0–4.0	28	25	28	35	14	38	168
Total	87	101	160	218	62	288	916

[a]Individuals in this dose category were exposed at distances in excess of 3 km from the hypocenter, and hence received doses that are substantially equivalent to zero. [b]Age at the time of the examinations that were conducted between 2004 and 2008.

Flow cytometry

Mononuclear cell fractions separated by the Ficoll-Hypaque gradient technique were analysed by three-colour flow cytometry using a FACScan flow cytometer (BD Biosciences, San Jose, CA, USA). Fluorescein isothiocyanate (FITC)-labelled HSCA-2 mAb was prepared as described previously (Kyoizumi et al. 2004). PerCP-labelled CD4 mAb and phycoerythrin (PE)-labelled CD45-related O (CD45RO) mAb were purchased from BD-PharMingen (San Diego, CA, USA) and Caltag Laboratories (Burlingame, CA, USA), respectively. Three different memory CD4 subsets were defined: $CD45RO^+$ cells that expressed higher (M1), intermediate (M2), and lower (M3) levels of CD43. For each donor specimen, the window for the M2 subset was set in a range where CD43 level was from ½- to 2-fold of the mean CD43 intensity for $CD45RO^-$ cells, and the windows for the M1 and M3 subsets were set just to the right and left sides of the M2 window, respectively (Figure 1). Note that this method of memory CD4 T-cell subset discrimination was established in a previous study (Ohara et al. 2002) in which functional and phenotypical differences among these subsets were characterised, using a gating procedure (i.e., that involved internal standardisation of fluorescence intensities) that avoided the effects of inter-experimental variability. The percentage of cells in the range of each subset was obtained in a total CD4 T-cell population.

Data analysis

Associations of the percentage of each memory CD4 T-cell subpopulation (*percentage*) with age at time of examination (*age*), gender (*gender*), and radiation dose (*dose*) were analysed using a multiple regression model (Armitage et al. 2002). The method assumed that the percentage of each T-cell subpopulation related to each explanatory variable in a log linear manner:

$$\log(percentage = \alpha + \beta_1(age - 70) + \beta_2 gender + \beta_3 does,$$

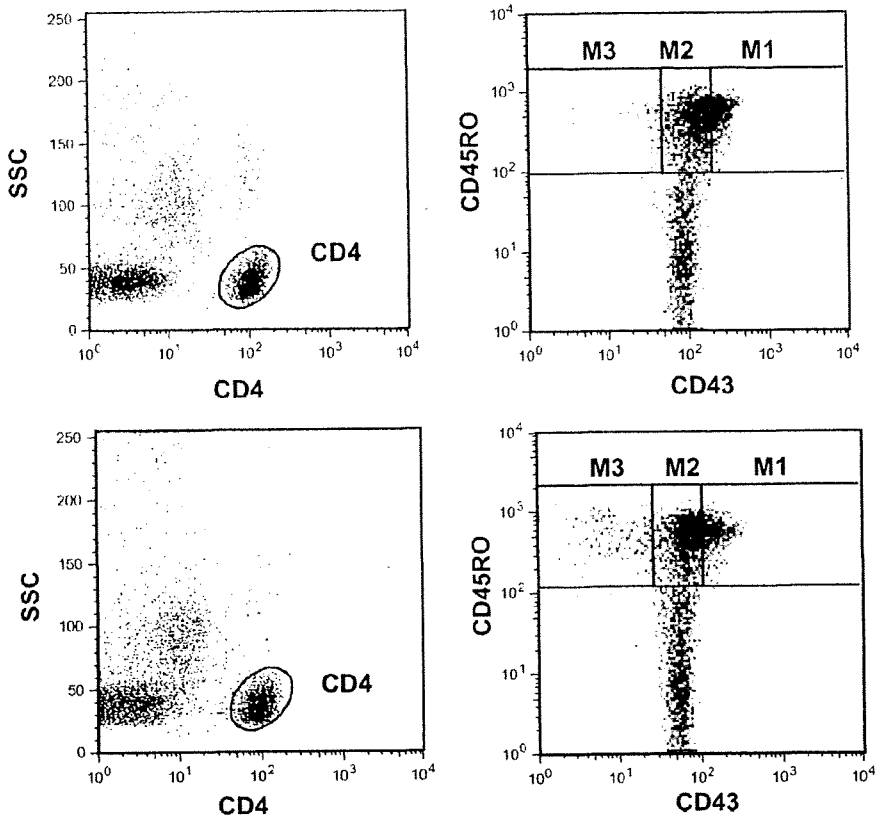

Figure 1. Flow cytometry patterns of CD4 T cells in the peripheral blood of 79-year-old females whose estimated radiation doses were zero (upper) and 0.525 Gy (lower). Peripheral blood mononuclear cells (about 2×10^5) were stained with FITC-labelled CD43 (HSCA-2) mAb, PE-labelled CD45RO mAb, and PerCP-labelled CD4 mAb. CD4 T cells were gated based on side light scattering (SSC) and CD4 intensity (left) and analysed for their expression of CD43 and CD45RO (right). Percentages of memory CD4 T-cell subsets in a total CD4 T-cell population of the unexposed were 24.1 for M1, 30.4 for M2, and 4.8 for M3, and those of the exposed were 17.2 for M1, 35.1 for M2, and 10.6 for M3.

where *gender* is an indicator of female sex, i.e., *gender* = 0 for male and *gender* = 1 for female, and *dose* is radiation dose in grays. The α is a constant term, and β_1, β_2, *and* β_3 are regression coefficients for variables to be estimated. The age term was subtracted by 70 years so that α corresponds to log-transformed percentage of CD4 T-cell subset, i.e., the subset percentage is calculated to be e^{α} (=exponential [α]), for non-irradiated males at 70 years of age. The % change of subset percentage was estimated to be $100(e^{10\beta_1}-1)$ per 10 years increment of age, and $100(e^{\beta_3}-1)$ per 1 Gy radiation dose. This regression analysis in the log linear manner was applied to evaluate the association of the percentage of memory subset within the CD4 T-cell population or CD45RO-positive memory CD4 T-cell population with age or radiation dose.

Results

Figure 1 shows the flow cytometry patterns of memory CD4 T-cell subsets within blood lymphocyte specimens of two age-matched women whose estimated exposure doses were zero and 0.525 Gy, respectively. Crude mean of percentage of each memory T-cell subset within the CD4 T-cell population was shown by age category and by dose category in Tables II and III, respectively. Table IV shows the association of the percentage of each memory T-cell subset with age and radiation dose, in terms of a multiple regression model. The percentage of memory cells (identified and enumerated by CD45RO-positivity) within the CD4 T-cell population appeared to significantly increase with age ($p < 0.0001$), and also with radiation dose ($p = 0.0060$). There was no difference in the percentage of CD45RO-positive memory cells between males and females (data not shown). As for memory T-cell subsets (M1, M2, and M3), the percentage of each subset in the CD4 T-cell population appeared to significantly increase with age ($p < 0.0001$); but again, these percentages did not differ between males and females (data not shown). The percentages of M2 ($p = 0.0001$) and M3 ($p = 0.0096$) subsets were found to significantly increase with radiation dose.

Table II. Crude means of the percentages of memory subsets in the CD4 T-cell population by age category.

	Age category		
	60–69 yrs	70–79 yrs	≥80 yrs
Subset	Mean 65.5 yrs	75.7 yrs	84.8 yrs
CD45 RO (total memory)	48.8 (1.10)[a]	52.2 (0.85)	58.1 (0.87)
M1 (mature, fully competent)	17.3 (0.62)	18.7 (0.49)	22.4 (0.56)
M2 (immature, poorly competent)	26.1 (0.57)	27.4 (0.43)	29.3 (0.45)
M3 (death prone, anergic)	5.3 (0.14)	6.1 (0.17)	6.4 (0.14)

[a]Standard error in parentheses.

Table III. Crude means of the percentages of memory subsets in the CD4 T-cell population by dose category.

	Radiation dose category			
	<0.005 Gy	0.005–0.5 Gy	0.5–1.0 Gy	1.0–4.0 Gy
Subset	Mean 0.0 Gy	0.20 Gy	0.75 Gy	1.74 Gy
CD45 RO	53.3 (0.93)[a]	53.1 (0.99)	55.0 (1.49)	54.6 (1.13)
M1	19.8 (0.57)	20.1 (0.57)	20.0 (0.88)	19.3 (0.72)
M2	27.4 (0.47)	27.2 (0.51)	29.0 (0.75)	29.0 (0.57)
M3	6.1 (0.18)	5.8 (0.14)	6.0 (0.21)	6.3 (0.20)

[a]Standard error in parentheses.

Table IV. Association of the percentages of memory subsets in the CD4 T-cell population with age or dose (multiple regression analysis)[a].

	% change of subset percentage per unit	
Subset	Age (10 years)[b]	Dose (1 Gy)[c]
CD45RO	10.8	4.3
	(8.0, 13.5)[d]	(1.3, 7.3)
	$p < 0.0001$	$p = 0.0060$
M1	14.6	1.3
	(10.1, 19.1)	(−3.7, 6.2)
	$p < 0.0001$	$p = 0.61$
M2	7.3	5.8
	(4.7, 10.0)	(2.9, 8.7)
	$p < 0.0001$	$p = 0.0001$
M3	10.6	4.9
	(7.2, 13.9)	(1.2, 8.6)
	$p < 0.0001$	$p = 0.0096$

[a]Representative memory subset percentage (95% confidence interval) for non-irradiated males at 70 years of age was calculated to be 15.3 (13.9, 16.7) for M1, 24.8 (23.6, 26.0) for M2, and 5.1 (3.9, 6.4) for M3. Note that there was no significant difference in the percentage of total CD45RO-positive memory cells and that of each memory T-cell subset between males and females. [b]Effects of age were estimated for 10 years. [c]Effects of radiation dose were estimated for 1 Gy. [d]95% confidence interval.

These radiation dose-related changes of memory T-cell subsets observed within the CD4 T-cell population may also involve comparable changes within memory subsets of the CD45RO-positive CD4 T-cell population (Table V). The percentages of M1 and M2 subsets in the memory CD4 T-cell population appeared to significantly increase and decrease with age ($p = 0.0085$ and $p < 0.0001$), respectively. In association with radiation dose, there was a statistically significant decrease in the percentage of M1 subset within the CD45RO-positive memory CD4 T cell population ($p = 0.039$). The ratio of the M1 subset to the combined M2 and M3 subsets also significantly decreased with radiation dose ($p = 0.043$), in contrast to a significant increase in this ratio with age ($p = 0.0030$).

Discussion

Our previous study (Ohara et al. 2002) has clearly shown functional differences among M1, M2, and M3 memory T-cell subsets: Cells in the M1 subset have greater capacity to respond to recall antigens (such as tuberculosis purified protein derivative and tetanus toxoid) and to secrete interferon-γ and IL-4 than cells in either of the other subsets; the M2 subset is comprised of memory-type cells that are less mature than cells of the M1 subset, in terms of not only their memory cell function (i.e., recall antigen reactivity and cytokine-producing ability), but also in terms of their chromosomes' telomere length (longer telomeres); and the M3 subset, in contrast to the M2 subset, consists of cells that are anergic to TCR-mediated stimuli and prone to apoptosis. Therefore, an increase in the proportion of these functionally less competent T-cell subsets (i.e., M2 and M3) may

Table V. Comparable changes of memory subsets within CD45RO-positive memory CD4 T-cell population with age or dose (multiple regression analysis).

	% change of subset percentage per unit	
Subset	Age (10 years)[a]	Dose (1 Gy)[b]
M1	3.5	−3.0
	(0.9, 6.1)[c]	(−5.8, −0.2)
	$p = 0.0085$	$p = 0.039$
M2	−3.2	1.5
	(−4.6, −1.8)	(−0.6, 3.0)
	$p < 0.0001$	$p = 0.059$
M3	−0.2	0.6
	(−3.4, 3.0)	(−2.9, 4.1)
	$p = 0.91$	$p = 0.73$
Ratio [M1/(M2 + M3)]	6.1	−4.5
	(2.1, 9.0)	(−8.8, −0.1)
	$p = 0.0030$	$p = 0.043$

[a]Effects of age were estimated for 10 years. [b]Effects of radiation dose were estimated for 1 Gy. [c]95% confidence interval.

not be beneficial to the individual in terms of immunological memory to previously encountered foreign antigens. Such preferential expansion of M2 and M3 subsets may also imply an insufficient maturation of antigen-primed CD4 T cells to the fully memory-competent M1 subset within the individuals' immune system. A hypothesis on memory CD4 T-cell differentiation pathways is depicted in Figure 2. After antigen exposure, naive T cells may undergo repeated cycles of cell division and transformation into the premature memory stage M2 cells. The conversion of M2 cells into the fully functioning mature memory stage M1 cells also requires population doublings following antigen exposure. Replication of M1 cells in response to recall antigens is largely responsible for the maintenance of memory functions. M3 cells, by contrast, are likely to be cells that are approaching senescence, and may arise from fully mature M1 cells that have lost survival signals such as cytokine signalling. We can also suspect that premature M2 cells are directly transformed into death-prone M3 cells. Such putative differentiation pathways may be controlled by interaction of memory T cells with antigen-presenting cells and environmental cytokine conditions. Such circumstances of memory T cells are very important to properly maintain immunological memory. In the CD4 T-cell systems of A-bomb survivors, there are at least two possibilities that the differentiation from M2 to M1 cells may be insufficient, and that cell transit from M2 and M1 subsets to apoptotic-prone M3 populations may be enhanced. Effects of radiation on cellular and molecular mechanisms controlling the memory T-cell differentiation pathways remain to be investigated. Taken together, our results suggest that function and maintenance of helper T-cell memory in the immune system of A-bomb survivors might have been compromised, after A-bomb irradiation.

Our previous study has shown that proliferative responsiveness of memory CD4 T cells to recall antigens can be enhanced by triggering cell-surface CD43 molecules with HSCA-2 mAb in vitro (Kyoizumi et al. 2004). That suggests that CD43 molecules play a part in certain of the cell signalling events involved in memory T-cell activation. Further, it is likely that CD43 and CD28 mAbs act synergistically to stimulate CD4 T-cell response to TCR cross-linking in vitro, indicating the co-stimulatory function of CD43 in TCR-mediated activation processes (Kyoizumi et al. 2004). It has also been suggested in the mouse immune system that the up-regulation of CD43 expression can have a negative effect on activation-induced cell death of T cells (He and Bevan 1999). A recent study has indicated that CD43 molecules induce a signalling cascade that prolongs the duration of TCR signal-mediated cell proliferation and cytokine secretion,

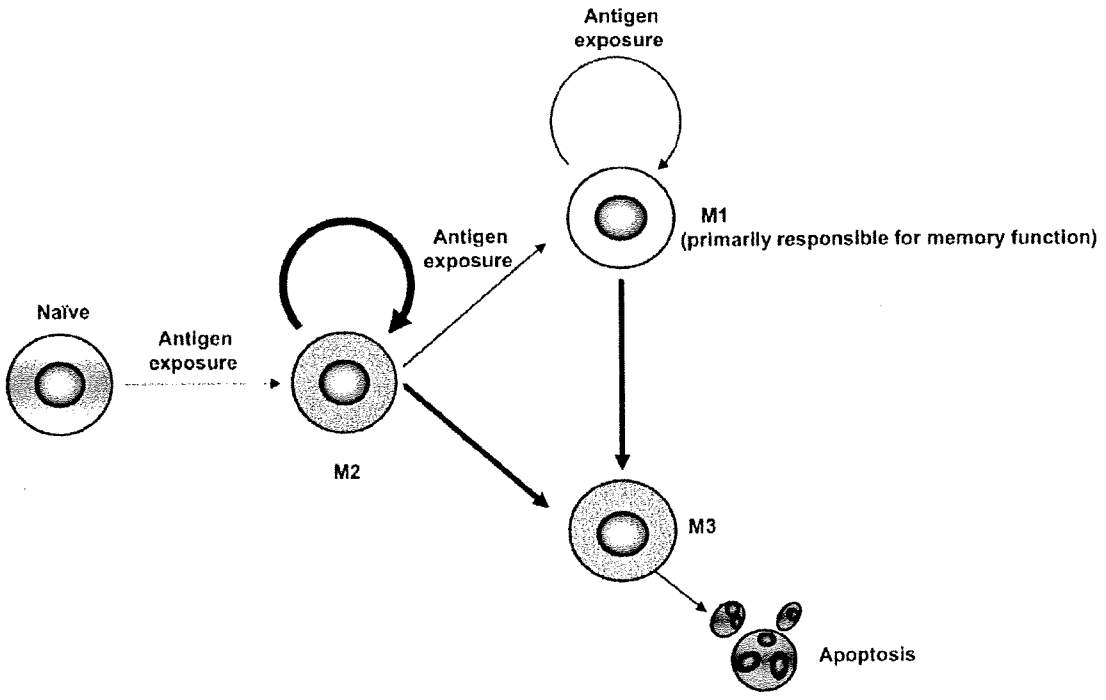

Figure 2. Hypothesised memory CD4 T-cell differentiation pathways for A-bomb survivors. Preferential pathways in the survivors' immune systems are drawn with bold lines.

but that prevents TCR signal-mediated anergy (Fierro et al. 2006). Thus, evidence is accumulating that there are positive effects of CD43-mediated signalling on activation and survival of memory T cells. By contrast, studies that have employed gene disruption techniques have shown that CD43 has either a negative regulatory role (Thurman et al. 1998, Tong et al. 2004), or possibly, plays no significant role in T-cell activation (Carlow et al. 2001). Although the precise mechanism of CD43-dependent regulation of T-cell activation remains to be determined, we have clearly demonstrated that CD43 expression is positively correlated with antigen responsiveness of memory CD4 T cells (Ohara et al. 2002). It is highly likely that the preferential increase in select memory subsets that express lower levels of CD43 (M2 and M3) may be associated with attenuated immune responses to specific pathogens. Levels of immunoglobulin G and A to *Chlamydia pneumoniae* have recently been found to decrease significantly with radiation dose among A-bomb survivors (Hakoda et al. 2006). It would be intriguing to study associations between antigen-specific responses to such ubiquitous pathogens and composition of memory T-cell subsets as defined by the relative level of CD43 expression among A-bomb survivors.

The individual's ability to properly maintain T-cell memory is known to decline with age (Goronzy and Weyand 2005, Weng 2006). This ageing-related immune attenuation is thought to be associated with: (i) The reduction in the size of naïve T-cell pool due to reduced production of new T cells within the involuted thymus, and subsequent, but infrequent entry of antigen-primed cells into the memory T-cell pool, and (ii) divergent antigen recognition repertoire of the memory T-cell pool due to the expansion or shrinkage of functionally incompetent memory T-cell populations (Goronzy and Weyand 2005, Weng 2006). Our previous observations of the immune system of A-bomb survivors are consistent with these typical features that relate to immunological ageing. In this regard, the proportion of naïve CD4 T cells was shown to decrease slightly, but significantly, with radiation dose (Kusunoki et al. 1998, 2002, Yamaoka et al. 2004). Also, the extent to which the TCR repertoire deviated from normal in memory CD4 T cells significantly increased with radiation dose in aged survivors (Kusunoki et al. 2003). An age-dependent increase in the percentage of M1 subset within the memory CD4 T-cell population may reflect the frequent expansion of functional memory T-cell populations in aged individuals. As far as we have examined for several individuals of the present study subjects, clonally expanded populations are largely distributed in M1 subset (Kyoizumi, manuscript in preparation), suggesting that, in aged individuals, only a small population of M1 subset may contribute to recall antigen responses in vivo. The observations in the present study can also be interpreted as an attenuation of helper T-cell memory possibly resulting from radiation-induced perturbation of T-cell homeostasis in A-bomb survivors.

Acknowledgements

The authors thank Dr Thomas M. Seed and Dr Evan B. Douple for careful reading of this manuscript. We are also grateful to Mika Yonezawa and Yoko Takemoto for their assistance with the manuscript preparation. The Radiation Effects Research Foundation (RERF), Hiroshima and Nagasaki, is a private non-profit foundation funded by the Japanese Ministry of Health, Labour and Welfare (MHLW) and the United States Department of Energy (DOE), the latter in part through the National Academy of Sciences. This publication was based on RERF Research Protocol RP 4-02 and supported in part by Grants-in-Aid for Scientific Research from Japan's Ministry of Education, Culture, Sports, Science, and Technology and MHLW.

Declaration of interest: The authors report no conflicts of interest. The authors alone are responsible for the content and writing of the paper.

References

Armitage G, Berry G, Matthews JNS. 2002. Statistical methods in medical research. Oxford: Blackwell Science.

Carlow DA, Corbel SY, Ziltener HJ. 2001. Absence of CD43 fails to alter T cell development and responsiveness. The Journal of Immunology 166:256–261.

Cullings HM, Fujita S, Funamoto S, Grant EJ, Kerr GD, Preston DL. 2006. Dose estimation for atomic bomb survivor studies: Its evolution and present status Radiation Research 166:219–254.

Dutton RW, Bradley LM, Swain SL. 1998. T cell memory. Annual Review of Immunology 16:201–223.

Eiraku N, Hingorani R, Ijichi S, Machigashira K, Gregersen PK, Monteiro J, Usuku K, Yashiki S, Sonoda S, Hall WW. 1998. Clonal expansion within $CD4^+$ and $CD8^+$ T cell subsets in human T lymphotropic virus type I-infected individuals. The Journal of Immunology 161:6674–6680.

Fierro NA, Pedraza-Alva G, Rosenstein Y. 2006. TCR-dependent cell response is modulated by the timing of CD43 engagement. The Journal of Immunology 176:7346–7353.

Fitzgerald JE, Ricalton NS, Meyer AC, West SG, Kaplan H, Behrendt C, Kotzin BL. 1995. Analysis of clonal $CD8^+$ T cell expansions in normal individuals and patients with rheumatoid arthritis. The Journal of Immunology 154:3538–3547.

Goronzy JJ, Weyand CM. 2005. T cell development and receptor diversity during aging. Current Opinion in Immunology 17:468–475.

Hakoda M, Kasagi F, Kusunoki Y, Matsuura S, Hayashi T, Kyoizumi S, Akahoshi M, Suzuki G, Kodama K, Fujiwara S. 2006. Levels of antibodies to microorganisms implicated in

atherosclerosis and of C-reactive protein among atomic bomb survivors. Radiation Research 166:360–366.

He YW, Bevan MJ. 1999. High level expression of CD43 inhibits T cell receptor/CD3-mediated apoptosis. The Journal of Experimental Medicine 190:1903–1908.

Kodama K, Mabuchi K, Shigematsu I. 1996. A long-term cohort study of the atomic-bomb survivors. Journal of Epidemiology 6(Suppl.):S95–105.

Kusunoki Y, Hirai Y, Hayashi T, Kyoizumi S, Takahashi K, Morishita Y, Kodama Y, Akiyama M. 1993. Frequent occurrence of in vivo clonal expansion of CD4 CD8 T cells bearing T cell receptor $\alpha\beta$ chains in adult humans. European Journal of Immunology 23:2735–2739.

Kusunoki Y, Kyoizumi S, Hirai Y, Suzuki T, Nakashima E, Kodama K, Seyama T. 1998. Flow cytometry measurements of subsets of T, B and NK cells in peripheral blood lymphocytes of atomic bomb survivors. Radiation Research 150:227–236.

Kusunoki Y, Yamaoka M, Kasagi F, Hayashi T, Koyama K, Kodama K, MacPhee DG, Kyoizumi S. 2002. T cells of atomic bomb survivors respond poorly to stimulation by *Staphylococcus aureus* toxins in vitro: Does this stem from their peripheral lymphocyte populations having a diminished naive CD4 T-cell content? Radiation Research 158:715–724.

Kusunoki Y, Yamaoka M, Kasagi F, Hayashi T, MacPhee DG, Kyoizumi S. 2003. Long-lasting changes in the T-cell receptor V beta repertoires of CD4 memory T-cell populations in the peripheral blood of radiation-exposed people. British Journal of Haematology 122:975–984.

Kyoizumi S, Kusunoki Y, Hayashi T, Hakoda M, Cologne JB, Nakachi K. 2005. Individual variation of somatic gene mutability in relation to cancer susceptibility: Prospective study on erythrocyte glycophorin A gene mutations of atomic bomb survivors. Cancer Research 65:5462–5469.

Kyoizumi S, Ohara T, Kusunoki Y, Hayashi T, Koyama K, Tsuyama N. 2004. Expression characteristics and stimulatory functions of CD43 in human $CD4^+$ memory T cells: Analysis using a monoclonal antibody to CD43 that has a novel lineage specificity. The Journal of Immunology 172:7246–7253.

Maini MK, Casorati G, Dellabona P, Wack A, Beverley PC. 1999. T-cell clonality in immune responses. Immunology Today 20:262–266.

Musette P, Bequet D, Delarbre C, Gachelin G, Kourilsky P, Dormont D. 1996. Expansion of a recurrent V beta 5.3^+ T-cell population in newly diagnosed and untreated HLA-DR2 multiple sclerosis patients. Proceedings of the National Academy of Sciences of the USA 93:12461–12466.

Nakano M, Kodama Y, Ohtaki K, Itoh M, Awa AA, Cologne J, Kusunoki Y, Nakamura N. 2004. Estimating the number of hematopoietic or lymphoid stem cells giving rise to clonal chromosome aberrations in blood T lymphocytes. Radiation Research. 161:273–281.

Ohara T, Koyama K, Kusunoki Y, Hayashi T, Tsuyama N, Kubo Y, Kyoizumi S. 2002. Memory functions and death proneness in three $CD4^+CD45RO^+$ human T cell subsets. The Journal of Immunology 169:39–48.

Posnett DN, Sinha R, Kabak S, Russo C. 1994. Clonal populations of T cells in normal elderly humans: The T cell equivalent to 'benign monoclonal gammapathy'. The Journal of Experimental Medicine 179:609–618.

Silins SL, Cross SM, Krauer KG, Moss DJ, Schmidt CW, Misko IS. 1998. A functional link for major TCR expansions in healthy adults caused by persistent Epstein-Barr virus infection. The Journal of Clinical Investigation 102:1551–1558.

Thurman EC, Walker J, Jayaraman S, Manjunath N, Ardman B, Green JM. 1998. Regulation of in vitro and in vivo T cell activation by CD43. International Immunology 10:691–701.

Waase I, Kayser C, Carlson PJ, Goronzy JJ, Weyand CM. 1996. Oligoclonal T cell proliferation in patients with rheumatoid arthritis and their unaffected siblings. Arthritis & Rheumatism 39:904–913.

Tong J, Allenspach EJ, Takahashi SM, Mody PD, Park C, Burkhardt JK, Sperling AI. 2004. CD43 regulation of T cell activation is not through steric inhibition of T cell-APC interactions but through an intracellular mechanism. The Journal of Experimental Medicine 199:1277–1283.

Wack A, Cossarizza A, Heltai S, Barbieri D, D'Addato S, Fransceschi C, Dellabona P, Casorati G. 1998. Age-related modifications of the human alphabeta T cell repertoire due to different clonal expansions in the $CD4^+$ and $CD8^+$ subsets. International Immunology 10:1281–1288.

Weng NP. 2006. Aging of the immune system: How much can the adaptive immune system adapt? Immunity 24:495–499.

Yamaoka M, Kusunoki Y, Kasagi F, Hayashi T, Nakachi K, Kyoizumi S. 2004. Decreases in percentages of naïve CD4 and CD8 T cells and increases in percentages of memory CD8 T cell subsets in the peripheral blood lymphocyte populations of A-bomb survivors. Radiation Research 161:290–298.

Radiation Research

Official Journal of the Radiation Research Society

Clonally Expanded T Lymphocytes from Atomic Bomb Survivors *In Vitro* Show No Evidence of Cytogenetic Instability

K. Hamasaki,[a,e] Y. Kusunoki,[a,e] E. Nakashima,[c] N. Takahashi,[b,e] K. Nakachi,[a] N. Nakamura[d] and Y. Kodama[b,e,1]

Departments of [a] Radiobiology and Molecular Epidemiology, [b] Genetics and [c] Statistics and [d] Chief Scientist, Radiation Effects Research Foundation, Minami-ku, Hiroshima, 732-0815, Japan; and [e] Hiroshima University Graduate School of Biomedical Sciences, Minami-ku, Hiroshima 734-8551, Japan

RADIATION RESEARCH 172, 234–243 (2009)
0033-7587/09 $15.00

DOI: 10.1667/RR1705.1

Clonally Expanded T Lymphocytes from Atomic Bomb Survivors *In Vitro* Show No Evidence of Cytogenetic Instability

K. Hamasaki,[a,e] Y. Kusunoki,[a,e] E. Nakashima,[c] N. Takahashi,[b,e] K. Nakachi,[a] N. Nakamura[d] and Y. Kodama[b,e,1]

Departments of [a] Radiobiology and Molecular Epidemiology, [b] Genetics and [c] Statistics and [d] Chief Scientist, Radiation Effects Research Foundation, Minami-ku, Hiroshima, 732-0815, Japan; and [e] Hiroshima University Graduate School of Biomedical Sciences, Minami-ku, Hiroshima 734-8551, Japan

Hamasaki, K., Kusunoki, Y., Nakashima, E., Takahashi, N., Nakachi, K., Nakamura, N. and Kodama, Y. Clonally Expanded T Lymphocytes from Atomic Bomb Survivors *In Vitro* Show No Evidence of Cytogenetic Instability. *Radiat. Res.* 172, 234–243 (2009).

Genomic instability has been suggested as a mechanism by which exposure to ionizing radiation can lead to cancer in exposed humans. However, the data from human cells needed to support or refute this idea are limited. In our previous study on clonal lymphocyte populations carrying stable-type aberrations derived from A-bomb survivors, we found no increase in the frequency of sporadic additional aberrations among the clonal cell populations compared with the spontaneous frequency *in vivo*. That work has been extended by using multicolor FISH (mFISH) to quantify the various kinds of chromosome aberrations known to be indicative of genomic instability in cloned T lymphocytes after they were expanded in culture for 25 population doublings. The blood T cells used were obtained from each of two high-dose-exposed survivors (>1 Gy) and two control subjects, and a total of 66 clonal populations (36 from exposed and 30 from control individuals) were established. For each clone, 100 metaphases were examined. In the case of exposed lymphocytes, a total of 39 additional *de novo* stable, exchange-type aberrations [translocation (t) + derivative chromosome (der)] were found among 3600 cells (1.1%); the corresponding value in the control group was 0.6% (17/3000). Although the ratio (39/3600) obtained from the exposed cases was greater than that of the controls (17/3000), the difference was not statistically significant ($P = 0.101$). A similar lack of statistical difference was found for the total of all structural chromosome alterations including t, der, dicentrics, duplications, deletions and fragments ($P = 0.142$). Thus there was no clear evidence suggesting the presence of chromosome instabilities among the clonally expanded lymphocytes *in vitro* from A-bomb survivors.

[1] Address for correspondence: Departments of Genetics, Radiation Effects Research Foundation, 5-2 Hijiyama Park, Minami-ku, Hiroshima 732-0815, Japan; e-mail: ykodama@rerf.or.jp.

INTRODUCTION

Radiation-induced genomic instability has been defined as events that occur in cells many generations after irradiation and that are distinguishable from the immediate effects of radiation. In 1992, Kadhim *et al.* (*1*) reported elevated frequencies of non-clonal *de novo* chromosome aberrations (mainly chromatid-type aberrations) in *in vitro* cultures of mouse hematopoietic stem cells irradiated *in vivo* with α particles. A number of delayed effects after exposure to both high- and low-LET radiation have since been described. It is now recognized that instability can be measured using not only chromosome alterations as a marker but also other end points such as gene mutations and cell death [see refs. (*2–5*) for reviews]. Genomic instability induced by radiation has been proposed to be an early event associated with the initiation of carcinogenesis (*6*). This model has therefore attracted many investigators interested in radiation-induced cancer.

While there are many reports describing radiation-induced genomic instability, only a few studies have been done with human cells, and the results are not concordant. Holmberg *et al.* (*7*) reported that the clonal descendants of X-irradiated human T lymphocytes acquired new stable-type aberrations 16–62 days after *in vitro* culture. In studies of people accidentally exposed to ^{137}Cs γ rays, Salomaa *et al.* (*8*) observed a significant increase in the frequency of exchange-type aberrations, including dicentrics (dic) in long-term lymphocyte cultures. Hofman-Huther *et al.* (*9*) observed an increased frequency of unstable-type aberrations (dic) at 8–41 days after the irradiation of human lymphocytes with X rays or 100 MeV/nucleon carbon ions. Similarly, delayed chromosome aberrations were reported in cultured human fibroblasts (*10–13*) and in human bone marrow cells (*14*). In contrast, Tawn *et al.* (*15*) examined lymphocytes from radiotherapy patients 6–60 months after their treatments and found no evidence for extended instabilities. Whitehouse and Tawn (*16*) did not detect any increase in the frequency of delayed chromosome alterations in the lymphocytes of radiation workers